RESEARCH TRIANGLE INSTITUTE

NASA CR-66891

AN ANALYTICAL INVESTIGATION OF ACQUISITION TECHNIQUES AND SYSTEM INTEGRATION STUDIES FOR A RADAR AIRCRAFT GUIDANCE RESEARCH FACILITY

By C. L. Britt, W. S. Thompson and L. S. Miller
Research Triangle Institute

Langley Technical Representative: W. L. Kitchen
Langley Research Center

Prepared under Contract No. NAS1-8912 by
RESEARCH TRIANGLE INSTITUTE
Research Triangle Park, N. C. 27709

for

NATIONAL AERONAUTICS AND SPACE ADMINISTRATION

January 1970

ACKNOWLEDGEMENT

This report was prepared for the National Aeronautics and Space Administration by the Research Triangle Institute under Contract NAS1-8912. It covers the first phase of a two phase study of a landing radar facility located at the NASA Wallops Station. This facility is used in the NASA Langley aircraft research programs which are primarily involved in VSTOL and STOL aircraft studies. The program is being administered by the Flight Instrumentation Division, NASA Langley Research Center. Mr. Wayne Kitchen of LRC is the Langley technical representative for the contract.

Messrs. Nathan Novack and Gene Godwin of NASA Wallops Station provided technical coordination and arrangements for instrumentation, personnel and range scheduling during the course of the flight tests. Mr. Donald Hines of RCA also provided invaluable assistance in connection with flight test instrumentation and test conduction.

This study was performed in the Engineering and Environmental Sciences Division at Research Triangle Institute. Dr. C. L. Britt served as project leader; Dr. L. S. Miller was engaged in early project planning and studying landing system requirements; Mr. W. S. Thompson participated heavily in system studies and report preparation; and Mr. R. C. Haws, Mrs. Christina Davis, and Mrs. Donna Nifong were all involved in computer programming and data analysis.

ABSTRACT

This report presents the results of a nine-month program conducted by the Research Triangle Institute with the following objectives: (1) determination of the runway instrumentation requirements at Wallops Station necessary to support present and proposed aircraft research programs from Langley Research Center, (2) evaluation of the status of the present radar equipment at Wallops Station and the feasibility of upgrading this equipment, (3) determination of any problem areas or basic limitations inherent in the present evolutionary runway instrumentation plans.

During the initial portion of the program, Langley runway instrumentation requirements were determined through interviews with aeronautical engineering personnel at LRC. A series of flight tests were then planned to determine whether or not the existing instrumentation was capable of meeting these requirements. During these tests, radar data was simultaneously obtained from the MPS-19, GSN-5, and the FPQ-6 radar systems located at Wallops Island. Magnetic tape and boresight camera data were also obtained during these tests, for various tracking modes and for both helicopter and fixed-wing tracking.

In general, the basic tracking accuracy of the GSN-5 radar was found to be within the expected accuracy bound. However, in comparisons of data output between radars, large discrepancies were noted in the computed x, y, z coordinates. These discrepancies cannot be attributed entirely to the GSN-5 because of the possibility of survey and geometrical errors that affect the accuracy of coordinate transformations.

Because of problems experienced in reliability and the flexibility demands of the experimental program, it is recommended that a more versatile radar system be obtained for use as the basic runway instrumentation equipment rather than funding a major modification of the GSN-5 equipment.

TABLE OF CONTENTS

Table of Contents (Continued)

I. SUMMARY AND RECOMMENDATIONS

The results of this study have led to the following general conclusions.

The basic tracking accuracy of the GSN-5, as evaluated through boresight camera records, is within the specified accuracy and expected performance for a radar of this type. The data taken during this phase did not permit a conclusive evaluation of the basic range tracking accuracy.

Analyses given in the text of this report show that the basic GSN-5 RMS angular tracking accuracy varies between 0.5 and 6 feet at one half mile range and between 2.5 to 5 feet at 2 1/2 mile ranges. These data were reduced from boresight camera records over five second intervals with a data rate of 16 samples per second. These figures represent the basic tracking capability of the GSN-5 and do not contain errors arising in the data processing, parallax correction and coordinate conversion subsystems.

Comparisons of position data outputs from the GSN-5 with those from the FPQ-6 radar indicated relatively large position errors. At a range (x) of 2 1/2 miles, the data errors for the beacon track mode were approximately 150 ft. (1.1%) in the x coordinate, 40 ft. in the cross range (y) coordinate, and 60 ft. (7%) in the altitude (z) coordinate. At 1/2 mile range, the x error reduced to approximately 20 ft. (.8%) and the y error was 40 ft. The altitude data at low altitudes was apparently not valid due to inaccuracies in low angle tracking by the FPQ-6 standard.

Since the data output comparison includes survey and geometric uncertainties, care should be taken in interpretation of these results. Further analyses of the form of the errors may indicate the error sources; however, time has not permitted this detailed analysis during the first phase of the program.

Pointing errors during slaving were found to be as high as 1.5° and frequent realignment is necessary. Slaving-aided acquisition was achieved in the test period somewhat less than 50% of the trials. The type of servo mechanism utilized in the GSN-5 is somewhat ill suited for slaving because of the several analog coordinate transformations required to provide slaving data in the proper form. It is felt, however, that with

more careful calibrations, the slaving performance can be improved over that noted during the test periods. The major cause of switchover transients is the large error in the slaving data.

Interviews with LRC project personnel using the radar system indicated that accuracies of $\pm$ 2 ft. in the last 1000 ft. before touchdown are required; that 360° tracking should be provided, and that there are no immediate requirements for digital output data. Reliability of the equipment is of major concern.

The principle limitations to the GSN-5 system are considered to be the low reliability and non-solid state design, acquisition problems, limited tracking range capability, and inaccuracies due to the analog data processing. Because of the age, reliability, and inherent design problems associated with the GSN-5, it is recommended that the possibility of acquiring other radar instrumentation be pursued. Factors which should be considered in the selection of another system are; digital processing (with both analog and digital readout) for greater accuracy and flexibility in glide slope simulation, long range 360° tracking capability, availability of beacons, and low system lags with tracking bandwidths of at least 10 Hz.

For accuracies of $\pm$ 2 ft. in the flare-out phase, optical laser or infrared (IR) should be investigated for use in conjunction with a lower frequency, all weather, long range radar. Long range plans should strongly consider use of a conventional radar augmented by an optical technique which is inherently free of ground environment multipath effects. It is recommended that in Phase II, existing, surplus, and new instrumentation be surveyed and analyzed as to applicability. The possibility of obtaining an FPS-16 as the basic radar should be strongly pursued.

II. INTRODUCTION

Langley Research Center, in connection with several of its flight instrumentation development programs, is a major user of the radar aircraft guidance facility at NASA-Wallops Station. These facilities are used to provide such diverse functions as the generation of ILS signals containing special non-linear glide slopes, and to provide rate signals via telemetry links to flight director equipment under development. The research-oriented nature of the facility requires that it meet a wide range of demands while providing reliable and accurate information for use in real time aircraft control.

The study reported herein was initiated by LRC in the interest of meeting the aircraft guidance requirements for their development programs over the next five-to-ten year span. The objectives of this study are to assess the requirements for existing capabilities, to identify needed improvement, to recommend courses of action, and to assist NASA in achieving the improvements. Work in the first phase (Phase I) of the study has been concentrated primarily on the identification of requirements and the evaluation of the existing radar system.

The present complement of equipment at Wallops Station comprises a GSN-5 and MPS-19 radar. The latter is a S-band radar which is used primarily for long range tracking and assisting the GSN-5 in acquisition. The GSN-5 is a 34 GHz system designed for accurate tracking and generation of ILS information. In a typical test, the GSN-5 will generate a 6° glide path for use with an STOL aircraft. The glide slope data is transmitted to the aircraft via a conventional ILS link. In other tests, the radar derived position information is telemetered to the aircraft for on-board computation and processing. Accuracies of $\pm$ 10 feet within 200 ft. of the touchdown point are acceptable for most of the aircraft programs. However, long range instrumentation plans should be based upon accuracies of plus or minus 2 ft. in the terminal landing phase. The aircraft test programs thus require high final-phase accuracy and the ability for continuous tracking or close-in acquisition of the landing trajectories.

The radars are positioned adjacent to the runway, and coordinate transformations are performed to refer the position and rate data (x, y, z coordinates) to a reference point (touchdown) on the runway. The GSN-5 uses analog computations and coordinate conversions throughout.

III. LANDING SYSTEM REQUIREMENTS

A. GENERAL

In order to identify the radar data requirements necessary to support NASA LRC studies, discussions were held with representatives from specific projects employing the radar aircraft guidance facility at NASA Wallops Station. NASA LRC personnel contacted in the initial investigation are identified by project in Table 3.1 which also includes specific statements in regard to data needs from the landing radar system. Several other general comments noted in discussions with other users and persons familiar with the current system operation are as follows:

(1) The accuracy of the system near touchdown after movement of the touchdown point during a series of tests appears to be degraded.

(2) Excessive fuel consumption and pilot fatigue frequently occurs because of required holding periods for equipment troubleshooting and revisions in system operation.

(3) Performance of the range servo is questionable, and it appears to oscillate at times.

(4) There appears to be considerable variation in day-to-day accuracy and performance.

It is emphasized that the findings listed in Table 3.1 only represents the needs of ongoing projects. In order to meet requirements over the next five to ten year span, some extrapolation of needs must be done.

A summary is given below in regard to capabilities needed to support ongoing programs.

B. SUMMARY OF REQUIREMENT

1. Accuracy

The most stringent equipment requirement was found to be the need for position data accurate to ± 2 feet in the last 1,000 feet before touchdown. With the anticipated development of Category III Landing Systems and the subsequent evaluation required of such systems, and the need for high accuracy during flare out, the 2 foot requirements are considered realistic.

Table 3-1. Summary of Contacts and Findings in Study of Landing Radar Requirements.

Project	Contact	Statement of Needs				Noted Problems
		Accuracy	Digital Data	360° Capability	Other Comments	
IFR Pilot Information	R. E. Dunham	±2 ft. for R < 1K ft.	Not Needed			0.5 sec. lag in output data
Graphic Glide Slope Indicator	R. E. Dunham			Not mandatory	Rate data needed	Break-lock frequently occurred
CH-46C Handling Qualities	F. R. Niessen	± 10 ft.	Would be helpful	Not Needed	Beacon tracking needed	TM rate data was bad--now being generated in aircraft from TM x, y, z
P-1127 Research on Deflected Jet	S. A. Morello	± 10% for R > 200 ft. ± 10 ft. for R < 200 ft.	Would be helpful	Strongly needed	Needs lightweight beacon	
XC-142 Terminal Area Flight test	H. Kelley	Published values adequate		Needed	Beacon tracking desirable	
Vector Analog Computer Display System	G. Culpepper				MPS-19 data is adequate	
A/C Noise Abatement	D. Maglieri	± 5%	Would be helpful	Not needed		

2. Digital Output

Even though there are no immediate program needs for digital output capability, digital processing is needed to provide the flexibility and accuracy anticipated for future systems. The requirement for a 2 foot accuracy at a 1,000 foot range is considered to be only marginally within the capabilities of operational analog hardware. If digital processing is used,it will be necessary to provide digital to analog conversion on the output in order to achieve compatibility with existing aircraft instrumentation.

3. 360° Tracking

There was only one specific incidence in which this capability was needed on present programs, however, there are operational reasons why this capability should be provided. Flexibility, continuity of data, the elimination of acquisition problems, less set-up time, and needs of changing flight paths are more than sufficient justification. As discussed in a later section of this report, the present slaving arrangement between the GSN-5 and the MPS-19 is considered only marginal for existing needs.

4. Beacon Tracking

Even though radar operation in the skin tracking or corner reflector tracking modes will continue to suffice for many programs, beacon tracking is considered necessary to achieve long range, low angle tracking with the 34 GHz equipment. At present beacon availability for the GSN-5 is extremely limited. On the P-1127 aircraft program, a beacon is needed with a maximum weight not to exceed 20 lbs.

5. Reliability

The time lost in test delays and cancellations with the present system due to acquisition failures, broken lock, and equipment failures is judged to be extensive. Intensive maintenance would be necessary to improve this situation because of the age and vacuum tube nature of the GSN-5 equipment. Because of weather, costs and range committments associated with aircraft test programs, reliability of the instrumentation is of utmost importance.

C. DETAILED PROGRAM REQUIREMENTS

The following requirements are based on interviews with the listed program personnel

Program No.1 ; Pilot Instrument Display for 0/0 Conditions

Contact: R. E. Dunham

Remarks:

1) Digital data is not needed.
2) An accuracy of 2 feet in the last 1000 feet is desired.
3) The 1969 test program has been completed.
4) Tests have shown a 1/2 second lag in GSN-5 data.

Program No. 2; Evaluation of Glide-Slope Displays

Contact: R. E. Dunham

Synopsis:

The objective of the program is to develop improved helicopter and V/STOL landing displays such as TV monitors and moving map instruments. Landing approaches under IFR conditions are presently limited to breakout ceilings of 200 feet or greater. As the approach path is steepened, airspeed must be decreased with an attendant deterioration in controllability. The instrument display problem is therefore much more critical for steep approaches. The information used in the presentation is derived from a guidance system consisting of GSN-5 radar data, ground-to-air telemetry, and an airborne analog computer.

Remarks:

1) An IP acquisition system is used, therefore 360° tracking is not mandatory.
2) A two-segment (3° and 6°) approach is used.
3) Rate information is needed.
4) GSN-5 has been modified for tracking out to 10 miles.
5) Lock-on problems have been troublesome with the GSN-5.

Program No. 3; Precision Approach Study Using CH-46-C and Y-HC-1A

Contact: F. R. Niessen

Synopsis:

The capability of the pilot to track flight director commands during concave downward approach paths will be assessed. The flight director information is developed as follows: X,Y and Y data from the GSN-5 is telemetered to the aircraft which contains TR-10 and TR-48 analog computers. Rate data is obtained by analog differentiations (in the aircraft) and control commands C are generated such as:

$$C_\theta = K_1 \theta + K_2 \dot{\theta} + K_3 \dot{X} + K_4 \delta (\theta)$$

where θ = pitch angle, and δ is pilot control input.

Flight Paths: Approach paths from a maximum range of 2 miles.

Remarks:

1) Does not need 360° tracking.
2) Digital radar data tapes would be helpful.
3) Would like to have telemetered X,Y, and Z. Present radar rate data is bad.
4) Position data should be accurate to less than 10 feet. A corner reflector is presently used.
5) Because of acquisition and track difficulties, should use a K-band beacon (weight no problem).

Program No. 4; Research on VTOL Fighter Aircraft

Contact: S. Morello

Remarks:

1) Definitely needs 360° and long range tracking.
2) Digitized data would be helpful.

3) Needs K-band beacon - weight problem - needs present corner reflector location for a camera.

4) Accuracy requirements

$\pm$ 10 ft. for R < 200 ft.; $\pm$ 10% for R > 200 ft.

Program No. 5; Terminal Area Flight Tests Using an XC-142

Contact: H. Kelley

Synopsis:

The program involves a study of terminal area flight problems peculiar to tilt-wing aircraft. The aircraft approach is cruise, or base-leg, to touchdown using an ILS receiver and flight director. A chase aircraft is used and published accuracy of the GSN-5 is considered adequate.

Remarks:

1) A K-band beacon is highly desirable.
2) 360° tracking is needed.
3) Accurate track-data is needed out to 5 miles range.
4) X, Y, and Z data is telemetered to the aircraft.

Program No. 6; Vector Analog Computer Display System

Contact: D. Culpepper

Remarks:

1) MPS-19 data is adequate.
2) Program to be finished 3-20-69.

Program No. 7; Noise Abatement

Contact: D. Maglieri

Synopsis:

The tests involve acoustic measurements under the following flight conditions:

a) level flight 200-500 feet.

b) hovering at 200 feet.

c) descent flares of 6-15-25 degrees.

Remarks:

1) Accuracy requirements are minimal, $\pm$ 5%.

2) Digital tapes would be helpful.

3) 360° tracking not needed.

IV. EXISTING SYSTEM DESCRIPTION

A. TOTAL SYSTEM

A block diagram of the system is shown in Figure 4-1. The heart of the system is the GSN-5 radar. The MPS-19 radar has been (recently) added to provide a 360° tracking capability and to assist the GSN-5 radar in acquisition when the target comes within the range and maximum look angle of the GSN-5.

The geometry of the radar guidance system is illustrated in Figure 4-2 for a particular set-up (for east-to-west approaches) with a general indication of the relative position of the MPS-19 and GSN-5 radars. Brief descriptions are given below for each of these radars.

B. GSN-5 RADAR

The basic unit is a pulsed, conical-scan, Ka-band, radar with analog outputs. Two trailer-mounted radars are available, both of which can be (simultaneously but usually only one-at-a-time) controlled remotely from a console housed in a van which also houses recorder, data link transmitters and special purpose equipment. A separate van also houses the equipment for powering the system. Specific technical characteristics are listed in Table 4-1.

The GSN-5 was originally designed as a landing control radar to provide either (1) total automatic landing control, (2) ILS signals, or (3) ground controlled approach (GCA) information. With several modifications, the radar facility has evolved into a general purpose, research-oriented data system adaptable to any number of special uses. Typical uses of the current system are:

(1) to provide tracking data for post test analysis,

(2) to provide ILS glide slope error and localizer signals for conventional glide slopes

(3) to provide ILS signals for special glide slopes and localizer paths,

(4) to provide position and rate data to the aircraft via a data link on a continuous basis.

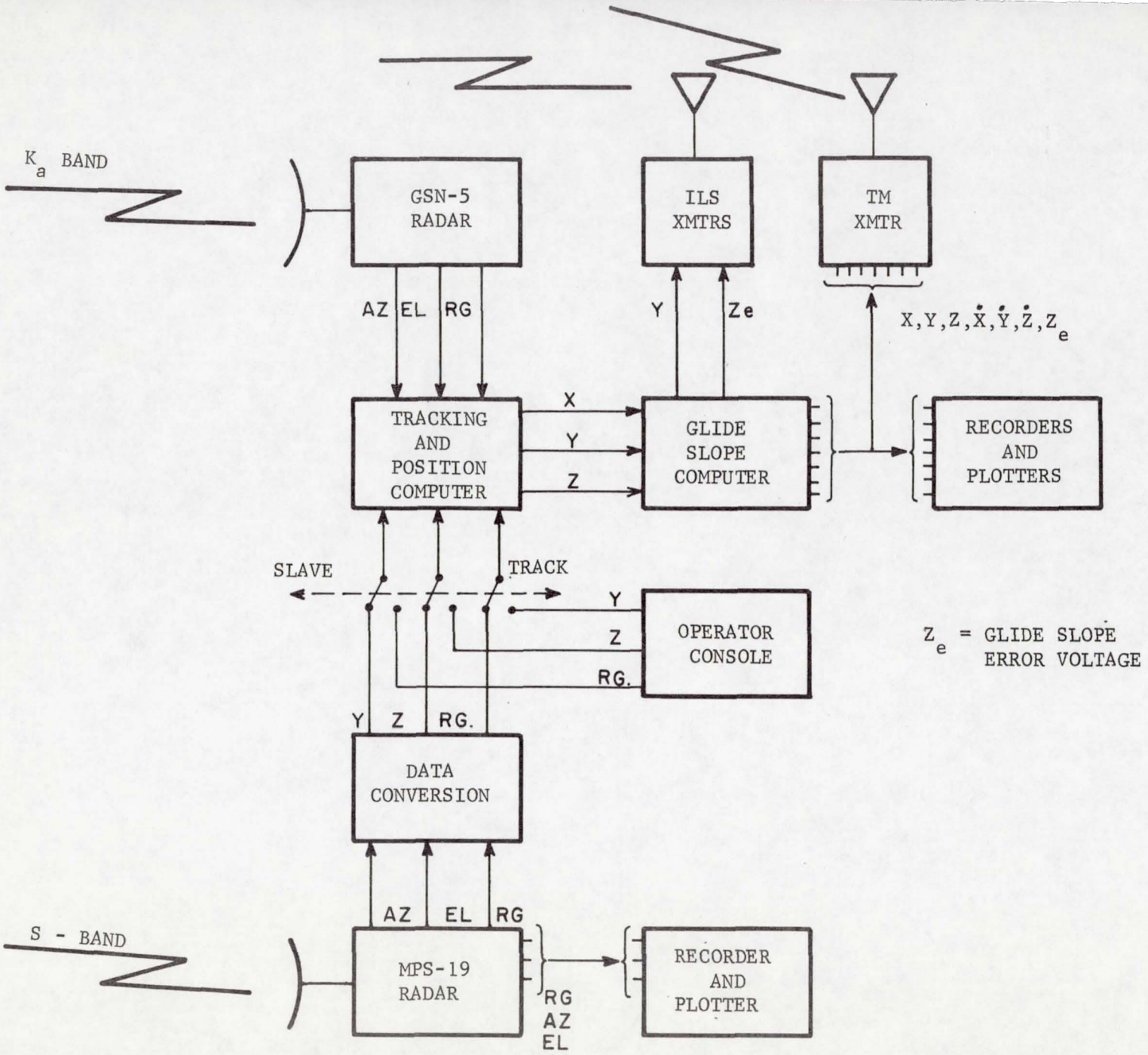

Fig. 4-1. System block diagram.

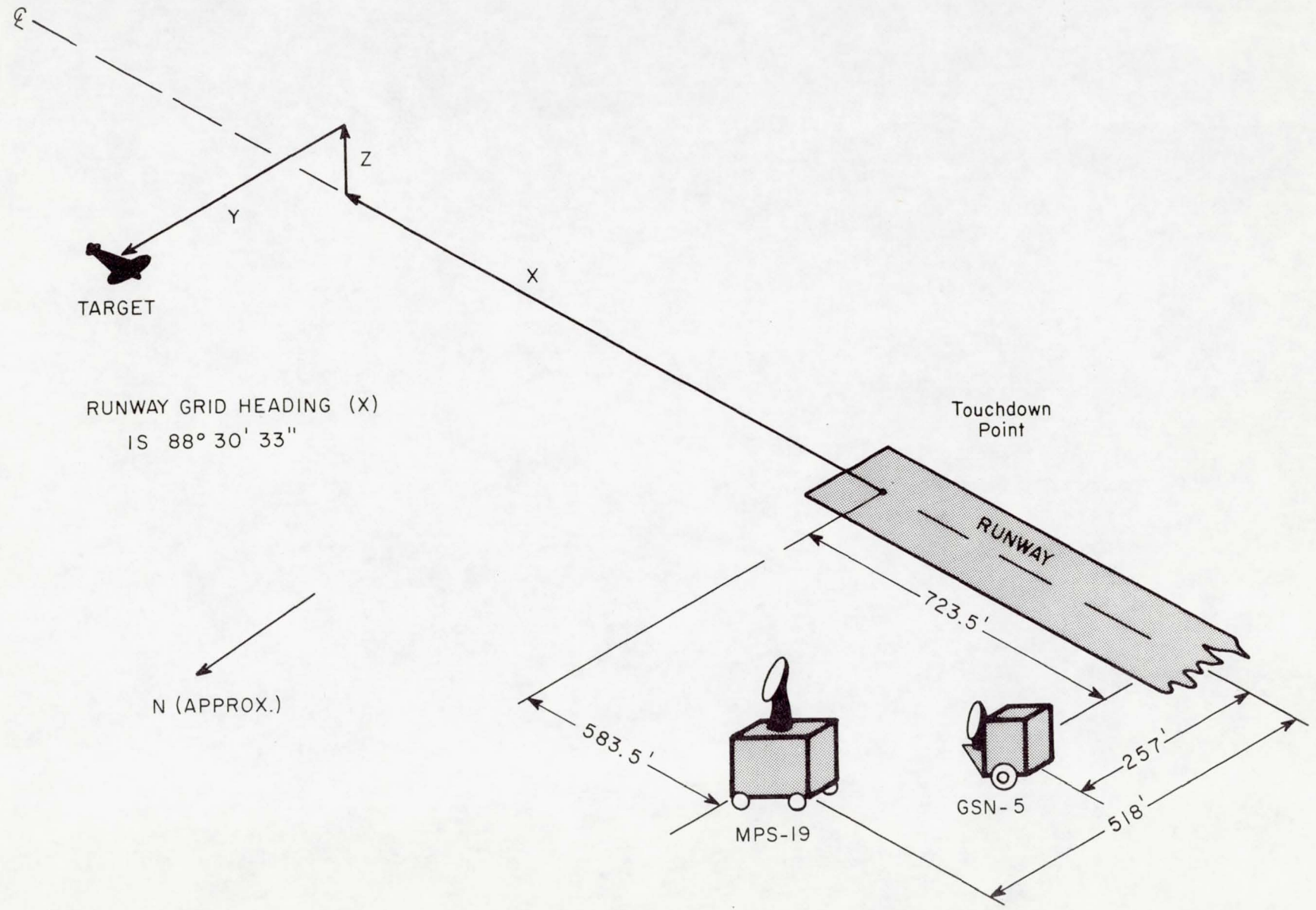

Fig. 4-2. Coordinate system and radar offsets.

Table 4-1. GSN-5 Technical Characteristics (Ref. 1)

Characteristics	Definition
Frequency	Radar operation: 34.860 ± 1% GHz. Beacon tracking: 33.200 ± 1 GHz for interrogate; 33.170 ± 1 GHz for receive
Pulse Width	0.2 μsec.
Pulse Repetition Rate	2000 pps.
Radar Peak Power	40 Kw.
Antenna Gain	48.5 db.
Receiver Sensitivity	-89 dbm.
Tracking Sensitivity	-80 dbm.
Maximum Range of Acquisition	Initially: 30,000 ft. modified to provide 3 settings of 30,000; 60,000; and 150,000 ft.
Minimum Tracking Range	300 ft.
Maximum Angles for Tracking	± 45 deg. in Azimuth + 30, -10 deg. in Elevation
Beamwidth	0.66 db. at -3 db. points
Conical Scan Rate	60 Hz.
Maximum Tracking Error (for 5 mile range)	15 ft. or 1%, whichever is greater, for x; 15 ft. or 1%, whichever is greater, for y; 1 ft. or 1%, whichever is greater, for z.

The GSN-5 is capable of tracking either in the vertical or circular polarization mode. Most of the tracking is done in the vertical polarization mode.

The radar is most often operated from a fixed position located approximately 250 ft. north of and 1500 ft. from the east end of the east-west runway, even though some special tests have required operation from other locations. Since the total look angle of the radar is only ± 45 degrees in azimuth the radar must be realigned for each change in aircraft approach direction.

For a fixed position the radar provides output voltages which are analogs of position coordinates in a cartesian reference system. Figure 4-2 illustrates the orientation of the coordinate system with the origin representing a specified touchdown point on the runway centerline. As the target is tracked a voltage proportional to range is supplied to the position computer which includes resolvers mounted on the antenna azimuth and elevation axes. The position computer performs a polar-to-cartesian coordinate conversion (range, azimuth, and elevation to x, y, and z) and applies offsets to these quantities for translation of the origin from the radar position to any specified point within certain limits.

C. MPS-19 RADAR

The MPS-19 radar is a part of an AN/MSQ-1 bomb scoring system. This radar is a member of the family of radar tracking instruments based upon the World War II radar,SCR-584. The radar is a conical scan, S-band radar with a 3° beam width. Table 4-2 summarizes the technical characteristics of the radar.

The antenna position control servo in the radar is a conventional zero velocity error system, with a tachometer feedback loop. A two-speed synchro system consisting of a 1:1 speed and 16:1 speed synchros is used for manually positioning the antenna and for analog data readout.

Table 4-2. MPS-19 Technical Characteristics (Ref. 2).

Characteristics	Definition
Frequency	2.700 to 2.900 GHz.
Pulse Width	0.8 μsec.
Pulse Repetition Frequency	Radar: 300 to 2000 pps. Beacon Tracking: 410 pps
Radar peak power	500 Kw.
Antenna Gain	34.5 db
Range (PPI Scales Listed)	50,000; 100,000; 200,000; 360,000 yds.
Minimum Range	500 to 1000 yds.
Maximum Angles for Tracking	360 deg. in Azimuth +89.5, -1.5 deg. in Elevation
Beam Width	3 deg. at -3 db points (with 8 ft. reflector)
Conical Scan Rate	30 Hz.
Tracking Accuracy (EST.)	3 mils RMS in angle 30 ft. RMS in range

V. FLIGHT TEST PROGRAM

A. GENERAL

To assess the radar tracking accuracies, a series of flight tests were planned during the summer of 1969. Several meetings were held with NASA-Wallops engineering personnel to arrange instrumentation and to schedule the flight tests.

Arrangements were made to have a boresight camera installed on the GSN-5 with provision for range timing, and to provide for analog magnetic tape and strip chart recordings of coordinate data from the GSN-5. In addition, digital magnetic tape recordings of parallax-corrected coordinate data were obtained from the MPS-19 radar at .1 second intervals. A Ka-band beacon was installed on a C-47 aircraft for tests requiring beacon capability.

Preliminary tests were conducted on May 23, 1969, using a helicopter. The purpose of this series of tests was to functionally check the instrumentation. Several problem areas were noted during these preliminary tests and corrected prior to the next series of tests.

Another series of tests were conducted on June 13, 1969, however, these tests were unsuccessful because of break-lock problems with the GSN-5 radar. As reported by the radar operator, W. Orr, the problem was discovered after the test were "scrubbed" to be due to phasing of the antenna-servo spin-error signal.

The tests were rescheduled for June 24, 1969; however, day to day postponements due to aircraft unavailability and weather resulted in a slippage to June 27. Difficulties with GSN-5 radar operation were also experienced on June 27, 1969, when the tests were conducted. Excessive jitter appeared in the azimuth and elevation channels; however, the cause, a bad vacuum tube in a line voltage regulator, was determined and corrected early enough to conduct a few tests on that day.

Another series of flight tests were conducted at Wallops Station on August 29, 1969. The major purpose of this series was to obtain tracking data for assessing the accuracy and performance of the GSN-5 radar in a Ka-band beacon tracking mode. Additional runs were conducted to check the consistency of data in linear and circular polarization tracking modes with those from previous tests, and to obtain additional data on GSN-5/MPS-19 slaving performance.

Two of three runs with the Ka-band beacon were satisfactory. The problem of oscillation in the GSN-5 slaving loop which appeared in previous tests was again encountered and prevented achievement of any runs involving radar slaving operation. Also, problems encountered with the boresight camera caused a loss of camera data in two of three runs using the linear and circular polarization tracking modes.

B. TEST PLAN

Two tests were used to provide for radar evaluation. The objectives, instrumentation, flight paths, and general plan for the two tests are summarized in the following:

1. Test No. 1: GSN-5 Radar Tracking Data Accuracy and Data Compatibility of the GSN-5 and MPS-19 Radars

Objective

1. To determine the accuracy of the tracking data from the GSN-5 in beacon and radar tracking modes.
2. To determine the suitability of the MPS-19 and GSN-5 systems for rapid data switchover in landing display systems.

General Test Plan

1. C-47 aircraft with C, K, and S band beacons and a corner reflector. Flight paths are specified in a separate section below. ILS inputs will be provided by the GSN-5 radar for all three runs. The K-band beacon operating modes during the three runs will be as follows:

Run No.	K-band Beacon Mode
A	OPERATE
B	STANDBY
C	STANDBY

2. GSN-5 with K-band beacon receiver and boresight camera with provision for recording (slow)* timing on the film. The radar will be set up for 5 n. mi. maximum tracking range. Tracking modes for the three runs will be as follows:

Run No.	GSN Tracking Mode
A	Beacon
B	Circular Polarization
C	Linear Polarization

Tracking and data acquisition will commence after the aircraft is within maximum tracking range as soon as acquisition is achieved and continue in to touchdown or until track is lost. Data outputs and recordings will be as follows:

a. XYZ, $\dot{X}\dot{Y}\dot{Z}$, and Z_e analog voltages supplied to the TM van.
b. XYZ, $\dot{X}\dot{Y}\dot{Z}$, and Z_e analog voltages and range (slow) timing recorded with the Sanborn strip chart recorder.
c. Y vs. X and Z vs. X analog voltages recorded with x-y plotters.
d. Magnetic tape recordings of ground-to-air and air-to-ground voice communications.
e. Boresight camera data.
f. ILS outputs to the aircraft.

3. MPS-19 beacon tracking on each run. Data acquisition will begin while the aircraft is 5.0 to 5.5 n. mi. down range and continue in to touchdown or until track is lost. Data outputs and recordings for all runs will be as follows:

a. Parallax corrected digital RAE output at 0.1 sec. intervals and range timing recorded on magnetic tape.

---

*"Slow" and "fast" range timing pertain to the NASA 28 bit and 36 bit codes respectively.

b. Parallax corrected Y vs. X and Z vs. X outputs plotted on x-y plotter.

c. Parallax corrected R, Y and Z (slaving) outputs to the GSN-5 also to be made available to the TM van.

4. FPQ-6 beacon tracking on each run. Data acquisition will begin while the aircraft is 5.0 to 5.5 n. mi. down range and continue in to touchdown or until track is lost. Data outputs and recordings for all runs will be as follows:

   a. Parallax corrected digital XYZ output at 0.1 sec. intervals and range timing recorded on magnetic tape.

5. The TM van contains a fourteen channel (not all of which will be used) FM recorder, a six channel strip chart recorder, and buffer operational amplifiers for receiving analog signals from the GSN-5 and driving the recorders. Data acquisition will begin while the aircraft is 5.0 to 5.5 n. mi. down range and continue in to touchdown or until track by the GSN-5 is lost. Data recordings for all runs will be as follows:

   a. Magnetic tape recordings of GSN-5 outputs XYZ, $\ddot{X}\ddot{Z}$, and Z_e and MPS-19 (slaving) outputs, R, Y, Z all from the buffer amplifiers plus range (fast) timing.

   b. Strip chart recordings of GSN-5 outputs XYZ and MPS-19 outputs YZ from the buffer amplifiers and range (slow) timing.

Flight Path (see Figure 5-1)

Runway: 28

Approach: East to West

Note: This runway and approach direction is required to provide minimum obstruction for tracking with the FPQ-6.

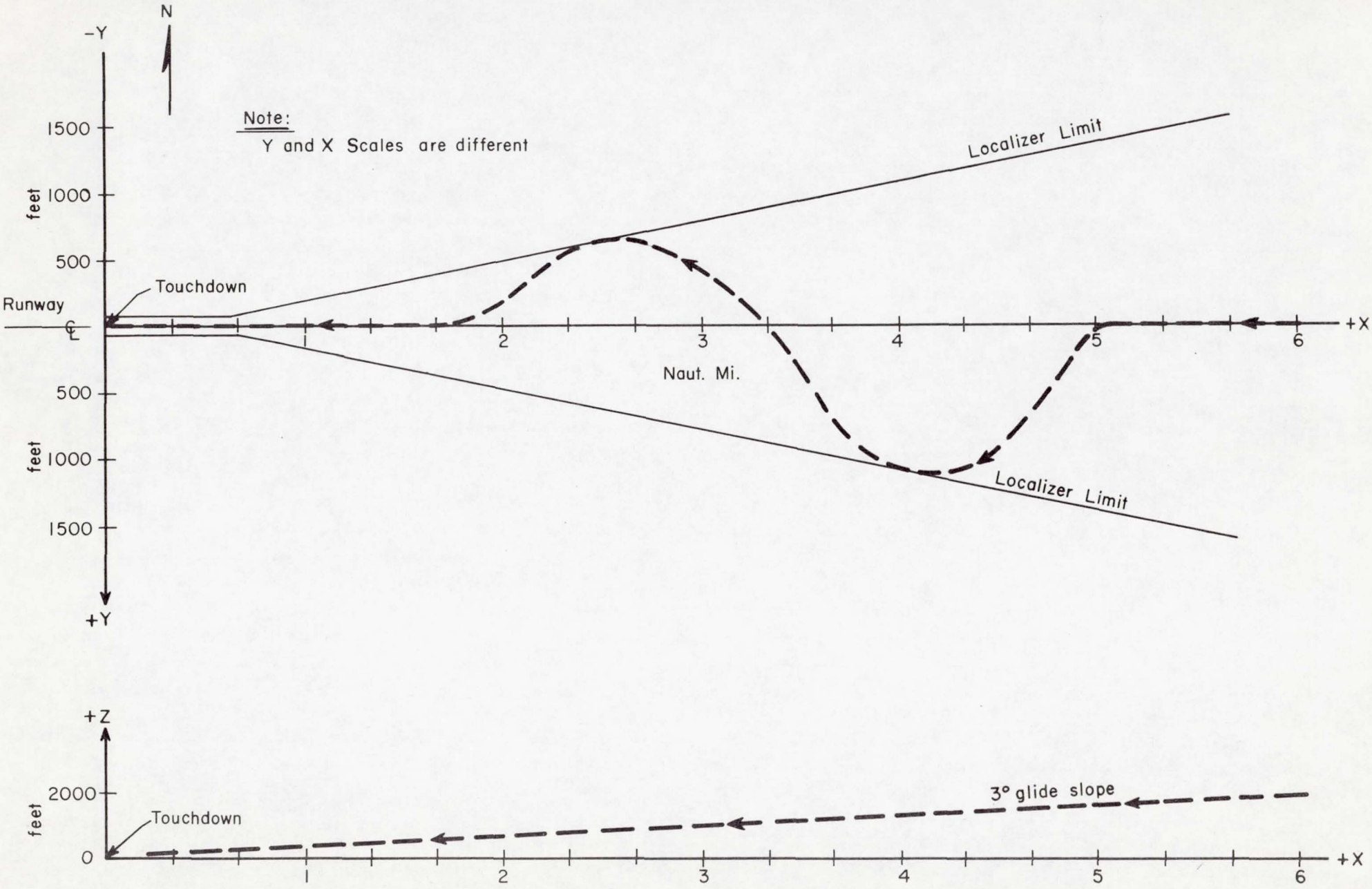

Figure 5-1. Flight path for test No.'s 1 and 2.

Glide Slope: 3 degrees

Starting Position: 6 n. mi. east of runway 28 and on the (extended) centerline of the runway and 1900 feet altitude. (This position is due east of Chincoteague High School over Oyster Bay.)

Initial Heading: West along the runway centerline.

Speed: Nominally 90 knots.

Course: From the starting position the aircraft will proceed in along the (extended) runway centerline and 3 degree glide slope. After GSN-5 lock-on (within 5 n. mi. downrange), the GSN-5 will provide ILS data. The aircraft will continue to follow the glide slope into touchdown. (Actual landing on each run is desired if weather conditions permit; otherwise, the landing will be aborted at the discretion of the pilot.)

Lateral zig-zag maneuvers are desired as illustrated in Figure 5-1. (Note that the y scale is greatly exaggerated in the diagram.) It is anticipated that the pilot can control the amplitude of the off-axis position by observing the localizer for maximum deflection. The positions of runway centerline crossover and maximum deviation from the runway centerline are not critical; the major requirement is to achieve some significant maneuver in both directions.

2. Test No. 2: GSN-5 Slaving and Switchover Performance Test

Objectives

1. To determine the GSN-5 data quality in the slaved mode.
2. To determine the nature and severity of transients during switchover.

General Test Plan

Three runs will be made each using the same aircraft and flight path as specified in Test No. 1. Only the GSN-5 and the MPS-19 radars will be used in this test (i.e., the FPQ-6 is not required for this test). The MPS-19 will be beacon tracking on all runs and will continuously generate slaving outputs to the GSN-5. The GSN-5 will be operated in different modes as specified below.

Instrumentation and Operation Requirements

1. C-47 aircraft with K and S band beacons and a corner reflector. Flight paths will be basically the same as specified for Test No. 1; however, the pilot will have to rely on visual (or any other available means) to stay on the flight path as the ILS signals from the GSN-5 will not be suitable due to unusual operations required of it during the test. The K band beacon operating status during the three runs will be as follows:

Run No.	K-Band Beacon Modes
A	STANDBY
B	STANDBY
C	OPERATE

2. GSN-5 with K band beacon receiver and boresight camera with provision for recording range (slow) timing on the film. The radar will be set up for 5 n. mi. maximum tracking range. Operating modes for the GSN-5 will be as follows:

Run No.	GSN-5 Operating Mode
A	Slaved mode throughout the run
B	Initially the slaved mode and then sequentially switched between slaved and corner reflector tracking modes (linear polarization) at approximately 20 sec. intervals throughout the run.

C	Initially the slaved mode and then sequentially switched between slaved and beacon tracking modes at approximately 20 sec. intervals throughout the run.

Data acquisition will commence when the aircraft is approximately 5 n. mi. down range and continue in to touchdown or until track is lost. Data outputs and recordings will be the same as items A through C specified for the GSN-5 radar in Test No. 1.

3. MPS-19 beacon tracking on each run. Data outputs acquisition will be the same as specified for the MPS-19 in Test No. 1.

4. TM van. Data acquisition will be the same as specified in Test No. 1.

Flight Path

The flight path for all runs will be the same as that specified for Test No. 1. As described under Instrumentation Item 1 above, the GSN-5 will provide ILS signals.

In addition to the two test summarized above, an additional test was conducted to measure the capability of the GSN-5 in following close-in aircraft maneuvers. For this test, a helicopter was used to perform maneuvers as directed during the test via ground-to-air voice links.

C. DATA REDUCTION

Data from the series of tests consisted of (1) boresight films, (2) digital tapes from the MPS-19 and FPQ-6 radars, (3) FM analog tapes from the GSN-5 radar, and (4) strip chart recordings from the GSN-5.

The boresight films were reduced at RTI. The digital magnetic tapes were processed by NASA-Wallops Data Processing Center to perform coordinate conversions to the GSN-5 position and to convert the tapes to the format requested by RTI. The analog tapes were processed at the NASA Langley Data Reduction Center to convert into digital form in the proper format. The strip chart recordings were shipped directly to RTI.

Initial inspection of the FM-recorded magnetic tapes indicated that the FM recorder was introducing 25 to 50 mv (approximately 125 to 250 millivolts peak to peak) of wideband noise, which even though significantly large was still within recorder specifications. Appropriate low-pass filtering of the analog output from the tape was used to remove the noise above 100 Hz.

VI. GSN-5 RADAR EVALUATION

A. RADAR POINTING ERRORS

Using developed film from the GSN-5 boresight camera, pointing errors were read from consecutive frames of selected portions of film for various GSN-5 tracking modes and targets, and RMS values computed. The reading methods and computation procedures are described in Appendix B.

Results of the GSN-5 tracking accuracy based on boresight camera data are presented in Tables 6-1 and 6-2. The values presented are RMS values of actual pointing errors computed from elevation and azimuth data read from 80 consecutive frames (approximately 5 seconds) for the selected cases of tracking mode and range shown. These data were obtained by a conventional variance analysis of values read off the boresight film. Estimates of reading errors and variance due to parallax contributions are also shown in Tables 6-1 and 6-2.

Table 6-2 shows that the RMS errors in the 12,000 - 15,000 range increment are in the order of 2 1/2 to 5 ft. Under short range conditions (2,600 ft.) angular errors vary from 0.5 to 3.8 ft. for both linear polarization and beacon tracking. The one exception is with circular polarization for which an error of 6 ft. was obtained. These data indicate that the tracking and servo portion of the radar were operating within expected bounds. In interpreting these results, it should be remembered that they represent typically the best accuracy that can be expected for the GSN-5 radar, i.e. these numbers represent the tracking accuracy if the data conversion from the tracking loop to the output were perfect. Also note that the data shown were computed from 16 sample per second data rates with a sample length of 5 seconds. Instantaneous excursions are, of course, much larger than the RMS values given.

Readings were taken at the two different ranges because of known differences in the operational configuration of the elevation and azimuth servo loops at these two ranges. Specifically, as range decreases past two miles, the servo systems are programmed to change from Type I to Type II servo configurations. The range intervals representing intermediate range

Table 6-1. GSN-5 RMS Pointing Error in Milliradians

Track Mode and Target	Designation of Result	Intermediate Range		Short Range	
		RMS Elev. Error, mils	RMS Az. Error, mils	RMS Elev. Error, mils	RMS Az. Error, mils
Linear Polarization C-47 Aircraft Corner Reflector on Aircraft (June 27 Test 1, Run C)	Total	0.20	0.19	0.22	0.32
	Reading Error	0.07	0.07	0.08	0.08
	Parallax Contribution	Negligible	Not Applicable	0.11	Not Applicable
	Residual	0.19	0.18	0.17	0.31
Linear Polarization C-47 Aircraft Corner Reflector on Aircraft (Aug. 29 Test 1, Run C)	Total			0.44	0.64
	Reading Error			0.06	0.06
	Parallax Contribution			0.11	Not Applicable
	Residual			0.42	0.63
Linear Polarization Helicopter Skin Track May 23 Test [b]	Total	0.27	0.32	0.61	1.46
	Reading Error	0.07	0.07	0.10	0.10
	Parallax Contribution	Negligible	Not Applicable	Negligible	Not Applicable
	Residual	0.26	0.31	0.60	1.46
Linear Polarization Stationary Corner Reflector (June 27, Pre-Test Calibration)	Total			0.14 [a]	0.16
	Reading Error			0.05	0.05
	Parallax Contribution			Negligible	Not Applicable
	Residual			0.13 [a]	0.15
Circular Polarization C-47 Aircraft Corner Reflector on Aircraft (June 27 Test 1, Run B)	Total	0.40	0.43	0.35	2.05
	Reading Error	0.09	0.09	0.05	0.05
	Parallax Contribution	Negligible	Not Applicable	0.12	Not Applicable
	Residual	0.39	0.42	0.32	2.05
Beacon Track C-47 Aircraft K_a Band Beacon on Aircraft (Aug. 29, Test 1, Run A)	Total	0.18	0.29	0.19	0.24
	Reading Error	0.05	0.05	0.06	0.06
	Parallax Contribution	Negligible	Not Applicable	0.002	Not Applicable
	Residual	0.18	0.29	0.18	0.23
Beacon Track C-47 Aircraft K_a Band Beacon on Aircraft (Aug. 29 Test 1, Run A)	Total	0.18	0.30		
	Reading Error	0.07	0.07		
	Parallax Contribution	Negligible	Not Applicable		
	Residual	0.17	0.29		

[a] Ground reflection may cause a bias in the absolute error which is not present in this reading.

[b] The May 23 helicopter tests were not part of the test plan described in Section V.B. but were special preliminary tests primarily for checking out recording systems.

Table 6-2. GSN-5 RMS Pointing Error in Feet

Track Mode and Target	Designation of Result	Intermediate Range			Short Range		
		Range (Kft)	RMS Elev. Error, ft.	RMS Az. Error, ft.	Range (Kft)	RMS Elev. Error, ft.	RMS A_z. Error, ft.
Linear Polarization C-47 Aircraft Corner Reflector on Aircraft (June 27 Test 1, Run C)	Total	12.8	2.6	2.5	2.6	0.6	0.8
	Reading Error		0.9	0.9		0.2	0.2
	Parallax Contribution		Negligible	Not Appl.		0.3	N/A
	Residual		2.4	2.3		0.5	0.8
Linear Polarization C-47 Aircraft Corner Reflector on Aircraft (Aug. 29 Test 1, Run C)	Total				2.6	1.2	1.7
	Reading Error					0.2	0.2
	Parallax Contribution					0.7	N/A
	Residual					1.1	1.7
Linear Polarization Helicopter, Skin Track May 23 Test [b]	Total	12.8	3.5	4.1	2.6	1.6	3.8
	Reading Error		0.9	0.9		0.3	0.3
	Parallax Contribution		Negligible	Not Appl.		Negligible	N/A
	Residual		3.3	4.0		1.6	3.8
Linear Polarization Stationary Corner Reflector (June 27, Pre-Test Calibration)	Total				1.075	0.2 [a]	0.2
	Reading Error					0.05	0.05
	Parallax Contribution					Negligible	N/A
	Residual					0.2 a/	0.2
Circular Polarization C-47 Aircraft Corner Reflector on Aircraft (June 27 Test 1, Run B)	Total	12.5	5.0	5.4	3.0	1.0	6.2
	Reading Error		1.1	1.1		0.2	0.2
	Parallax Contribution		Negligible	Not Appl.		0.4	N/A
	Residual		4.9	5.3		0.9	6.2
Beacon Track C-47 Aircraft K_a Band Beacon on Aircraft (Aug. 29 Test 1, Run A)	Total	15.5	2.9	4.6	2.7	0.5	0.7
	Reading Error		0.8	0.8		0.2	0.2
	Parallax Contribution		Negligible	Not Appl.		0.04	N/A
	Residual		2.7	4.5		0.5	0.6
Beacon Track C-47 Aircraft K_a Band Beacon on Aircraft (Aug. 29 Test 1, Run A)	Total	15.5	2.8	4.6			
	Reading Error		1.2	1.2			
	Parallax Contribution		Negligible	Not Appl.			
	Residual		2.5	4.4			

[a] Ground reflection may cause a bias in the absolute error which is not present in this reading.

[b] The May 23 helicopter tests were not part of the test plan described in Section V.B. but were special preliminary tests primarily for checking out recording systems.

were generally chosen to lie just beyond the two mile point. Short range intervals were chosen to lie at approximately one-half n. mi.

B. STATIONARY TARGETS

Two stationary targets were used for comparisons of radar data outputs with survey data. These were the corner reflector used for GSN-5 calibration and a water tower located approximately four miles from the GSN-5 position.

From survey data, the positions of these two reference points are (measured in the touchdown coordinate system):

	Survey Data		
	X	Y	Z
Water Tower	23841.67	-3449.65	-
Corner Reflector #1	351.0	255.0	≃7

Various data readouts from the GSN-5 on the corner reflector are summarized in Table 6-3.

Table 6-3. Comparison of survey and data outputs for GSN-5 locked on corner reflector #1. Units are ft.

	X	ΔX	Y	ΔY	Z	ΔZ
Survey	351		255.		7	
June 27 Pre-test	338	-13	255.	0	5	-2
June 27 Post-test	333	-8	254.	-1	1	-6
Aug. 29 Pre-test	340	-11	264.	+9	7	0
Aug. 29 Post-test	N.A.	--	259.	+4	8	+1

Note: ΔX, ΔY, ΔZ are differences between measured and surveyed values.

The data in the table represent measurements that were obtained from the GSN-5 data tapes, and the data were averaged over approximately 15-20 seconds.

One test was conducted with the water tower reference. However, it is felt that the GSN-5 was locked on some other target during this test. The coordinates measured are listed in Table 6-4. Comparison with survey data and inspection of the boresight film indicated that the target was most likely a large building rather than the water tower.

The FPQ-6 and MPS-19 radars did lock on the water tower, providing results as indicated in Table 6-4.

Table 6-4. Comparison of survey and measured data for FPQ-6 and MPS-19 locked-on water tower. Units are ft.

	X	ΔX	Y	ΔY	
Survey	23,842		-3450		
FPQ-6 Pretest	23,937	+95	-3593	-43	
FPQ-6 Post-test	23,879	+37	-3572	-22	
MPS-19 Pretest	25,187	+1345	-3371	-221	(slaving voltage output)
GSN-5*	24,353	+511	-2888	-562	

*Note: possibly locked-on building.

The large discrepancy between the FPQ-6 and MPS-19 is consistent with later tests discussed in Section VII. The MPS-19 output in this case was the slaving voltage to the GSN-5, not the digital output.

It should be noted that Table 6-3 and 6-4 data indicate the overall degree of repeatability and accuracy of the processed radar data outputs. This includes the calibration, analog recording, and digitization processes.

C. COMPARISON OF GSN-5 and FPQ-6 TRACKS

The x, y, z coordinate data for several test runs have been differenced and compared. The data outputs from the GSN-5 and FPQ-6 were synchronized in space and time in the touchdown coordinate system. Figure 6-1 shows the comparison between the FPQ-6 and GSN-5 data, for the GSN-5 in the linear polarization mode. This is Test 1, Run C, from the June 27 test series. The top traces indicate the absolute value of the x coordinate in feet for both the FPQ-6 and GSN-5 radars. Directly above the absolute value trace is the difference between the two tracks, also in feet. Also shown on the plot are similar curves for the y and z coordinates.

The radar positions are shown in the touchdown coordinate system in Figure 6-2. Note that a measurement in the x coordinate by the FPQ-6 corresponds to a measurement in range and azimuth by the FPQ-6 radar, whereas a measurement in y is, for the most part, a range measurement. Thus, from the FPQ-6 standard we would expect measurement accuracies of roughly 5 feet RMS in x and 9 feet RMS in y.

The differences between the GSN-5 and FPQ-6 in the x coordinate are approximately 200 feet at a range of 2 miles, reducing to zero and crossing over at a range of approximately 1.5 n. mi. In the y coordinate, there is an initial transient, possibly due to the recording technique, and then peak errors on the order of 45 feet occur. In the z coordinate, the errors are initially on the order of 80 feet and gradually reduce to zero. Towards the latter part of the run, the FPQ-6 apparently develops large errors in z due to extreme low angle tracking. The FPQ-6 data tend to level off at a z value of approximately 270 feet.

Figure 6-3 shows a similar set of curves for a repeat of Test 1, Run C from the August 29 series. In this test, the aircraft maneuvers were somewhat more extreme in the y coordinate than in the previous series of tests. The general behavior of the error in the x coordinate is similar to that in the June 27 test, as is the behavior in the z coordinate. In y, the peak error is consistent with a lag in the GSN-5 data output during the initial part of the run. Note that in this test, the FPQ-6 z data tended to level off at a value of roughly 350 feet.

GSN-5 X, FPQ-6 X, AND DELX VS TIME

GSN-5 IN LINEAR
POLARIZATION

SMOOTHED DATA

START TIME
176 DAYS, 16HRS,
43 MIN. 35.5 SEC

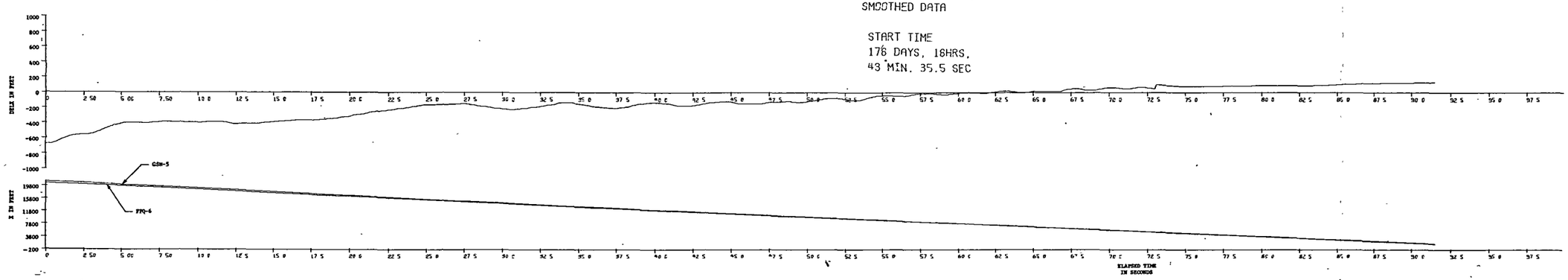

GSN-5 Y, FPQ-6 Y, AND DELY VS TIME

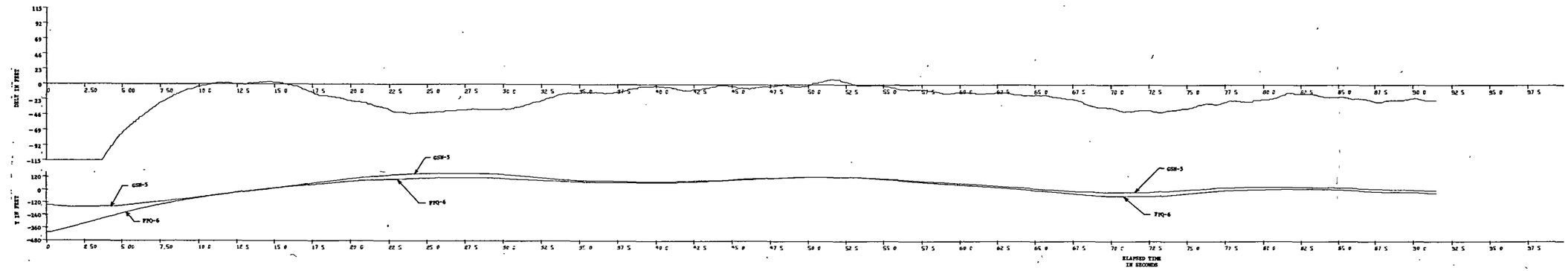

GSN-5 Z, FPQ-6 Z, AND DELZ VS TIME

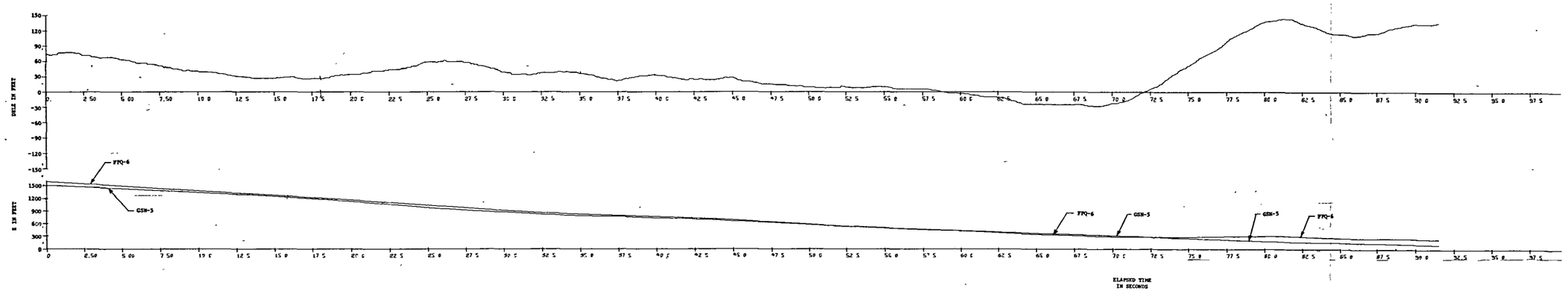

Figure 6-1. X, Y, Z coordinate data from the FPQ-6 and GSN-5 compared - Test 1, Run C, June 27. (Linear Polarization).

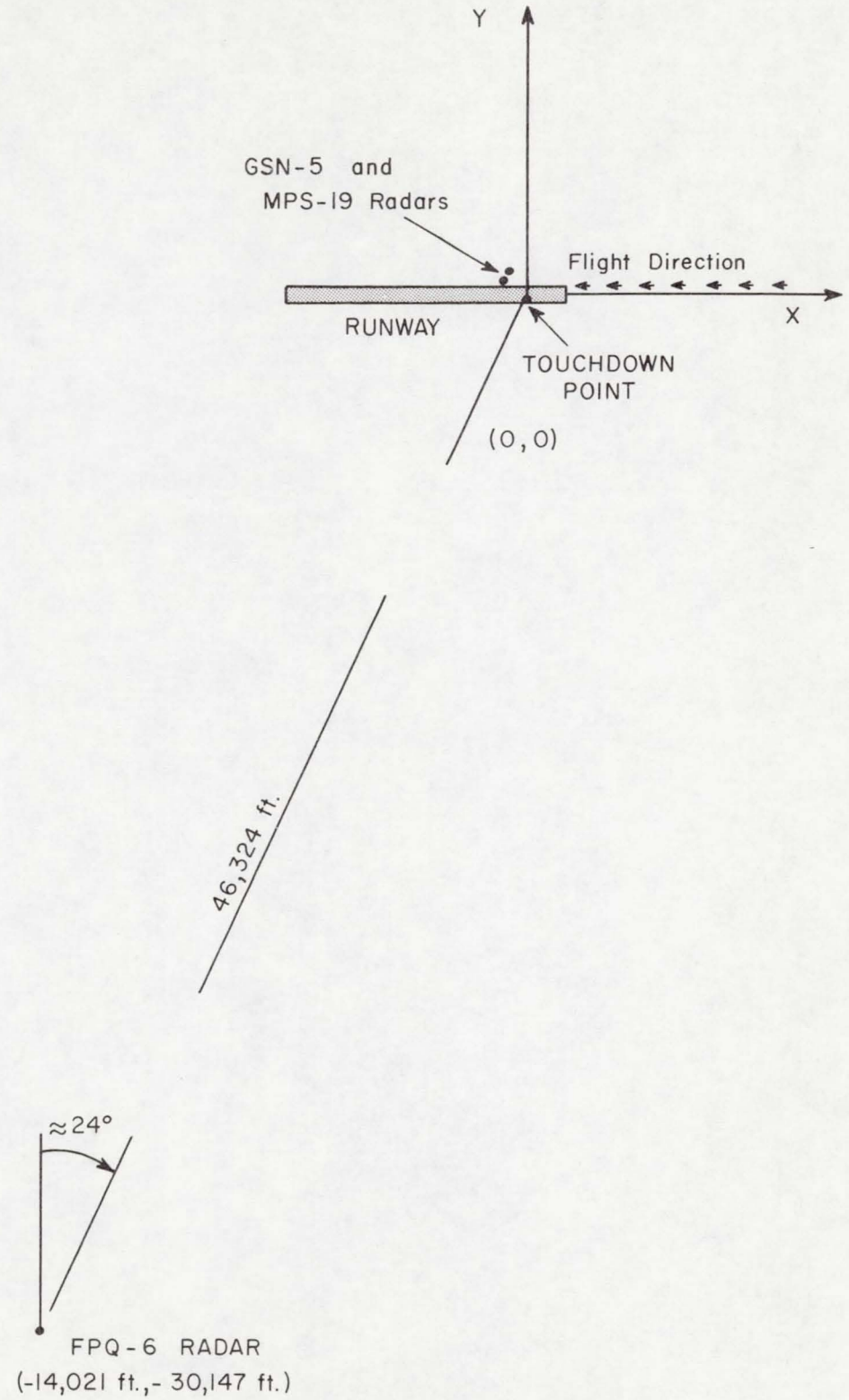

Fig. 6-2. Radar positions in touchdown coordinate system.

GSN-5 X, FPQ-6 X, AND DELX VS TIME

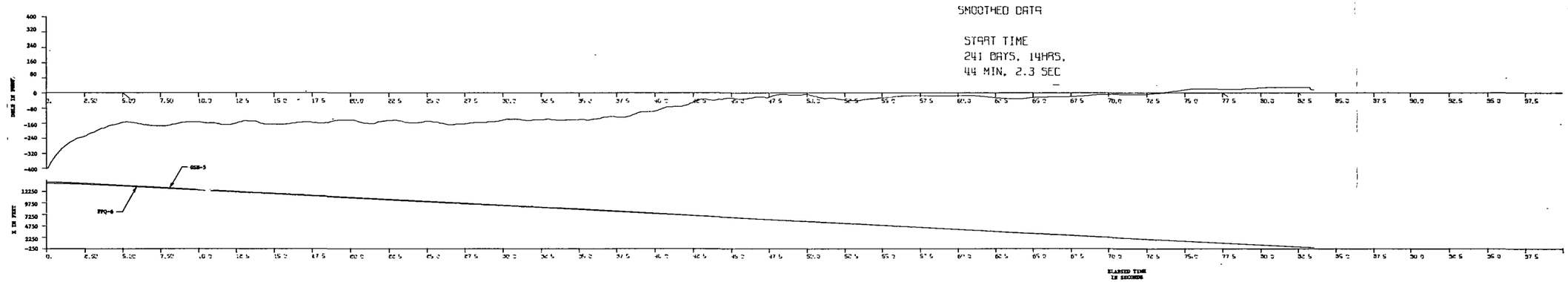

GSN-5 Y, FPQ-6 Y, AND DELY VS TIME

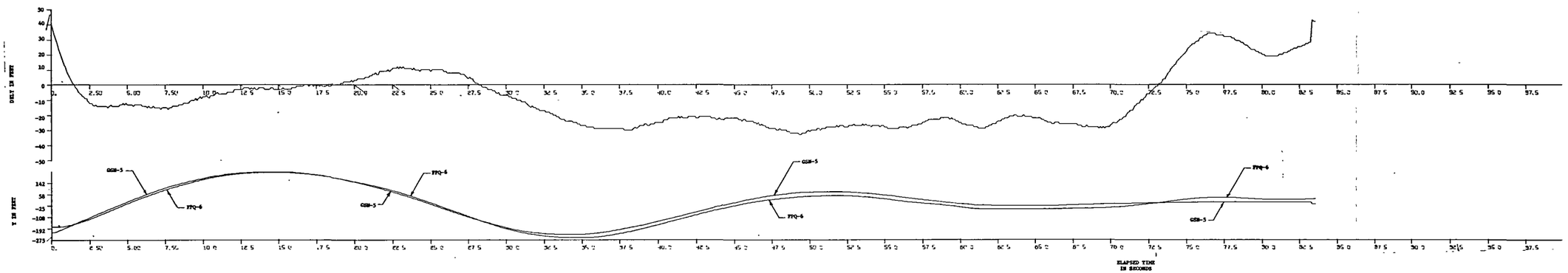

GSN-5 Z, FPQ-6 Z, AND DELZ VS TIME

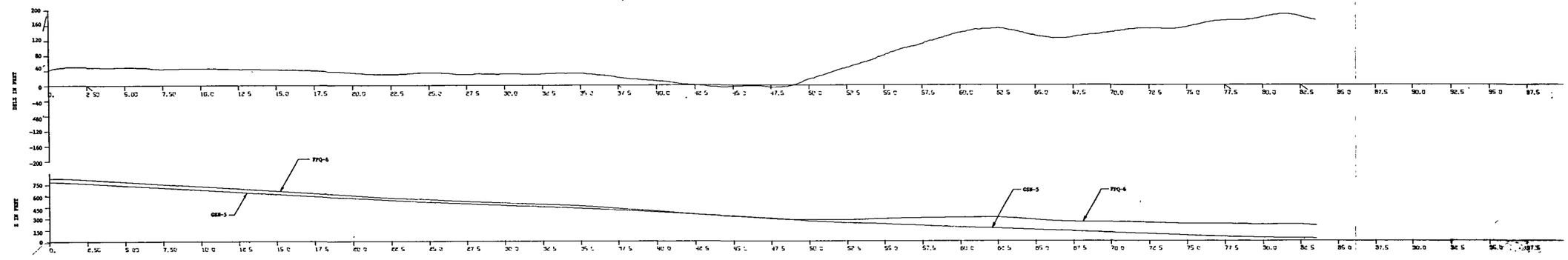

Figure 6-3. X,Y,Z coordinate data from the FPQ-6 and GSN-5 compared - Test 1, Run C (Repeated) August 29. (Linear Polarization).

Figure 6-4 shows the data from Test 1, Run A on August 29th. Again the behavior in the x coordinate is similar to the two previously discussed tests. Peak errors in the y coordinate are on the order of ± 30 feet and again the behavior of the data at the initial part of the run is consistent with a data lag in the GSN-5 output. Differences in z coordinate are initially 80 feet and gradually decrease to zero prior to the FPQ-6 data leveling off as in all previous test. Note that Test 1, Run A, was a test using the beacon track mode.

Because of the low angle track of the FPQ-6 radar, very little confidence can be placed in the z coordinate data. In all cases, the FPQ-6 data flattened out at an altitude on the order of 200-300 feet. The y data is felt to be the most accurate, since it corresponds to essentially a range measurement at the FPQ-6 when the aircraft is roughly 2 1/2 miles from the touchdown point. In the y data, no consistent bias offsets are evident that would be indicative of a survey error. We thus feel that the y data reflect the overall data accuracy of the GSN-5 data output, particularly at intermediate times during the various runs.

D. RELIABILITY

Major problems in the Wallops test programs are caused by GSN-5 breakdowns. During the test program discussed in this report, several breakdowns of the radar took place causing schedule slippages and missed data. For example, a series of test scheduled on June 13th failed because of break-lock problems with the GSN-5 radar. The problem was due to phasing of the antenna servo spin-error signal. Difficulties with GSN-5 radar operation were also experienced on June 25th when the tests were conducted. Excessive jitter appeared in the azimuth and elevation channels; due to a bad vacuum tube in a line voltage regulator.

On August 29th, a problem of oscillation in the GSN-5 slaving loop (which also appeared in previous tests) was again encountered and prevented achievement of any runs involving radar slaving operation.

GSN-5 X, FPQ-6 X, AND DELX VS TIME

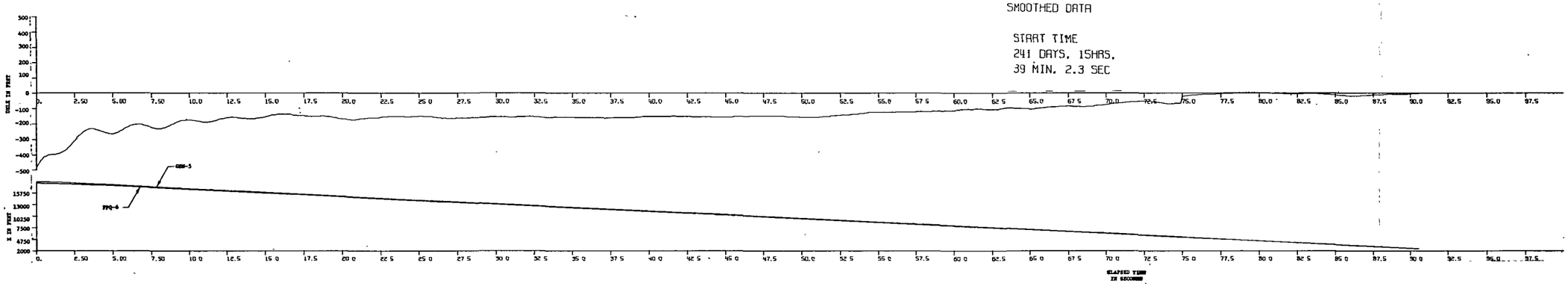

GSN-5 Y, FPQ-6 Y, AND DELY VS TIME

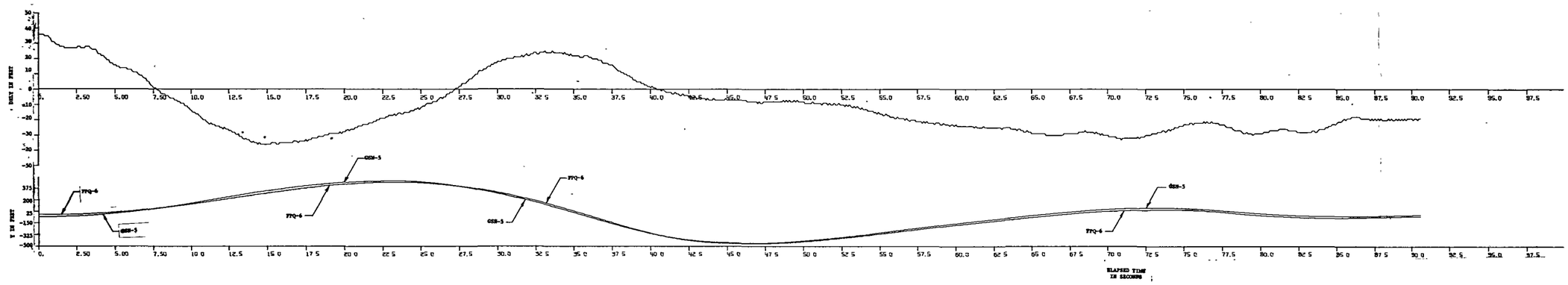

GSN-5 Z, FPQ-6 Z, AND DELZ VS TIME

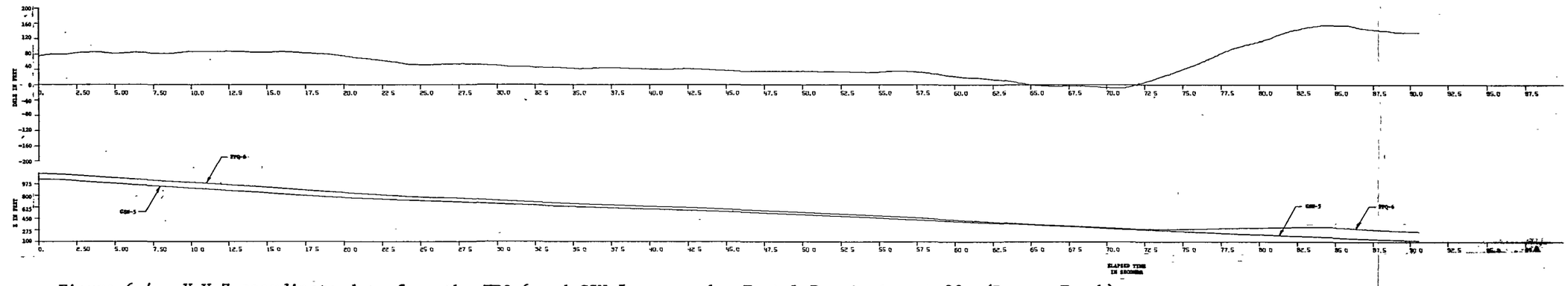

Figure 6-4. X,Y,Z coordinate data from the FPQ-6 and GSN-5 compared - Test 1 Run A, August 29. (Beacon Track).

The successful operation of the radar is highly dependent on the skill of the operator. As with most experimental radars, documentation of circuit changes has not been kept up to date and a complete diagram, including all modifications, is not available. Therefore, reliability problems can be expected to increase when the radar is taken over by new operators unfamiliar with the pecularities of the system.

VII. MPS-19/GSN-5 SLAVING PERFORMANCE

A. SLAVING TECHNIQUE

Because of the arrangements of the servo systems in the two radars, the slaving arrangement is relatively complex. The servo loop of the GSN-5 radar contains a resolver chain in the servo loop such that command signals are in x, y, z coordinates. A simplified block diagram of one channel of the GSN-5 servo arrangement is shown in Figure 7-1. As may be seen from the diagram, the elevation channel is driven by a z command voltage. Thus, the elevation angle achieved depends upon the command voltage (z), the slant range fed into the resolver chain, and the z offset voltage which is used for parallax correction. With the present synchro arrangement, it is not possible to derive voltage analogs proportional to elevation and azimuth.

The servo system of the MPS-19 is conventional, using elevation and azimuth command voltages to position the antenna. Both 1:1 and 16:1 synchro control transformers are used on the antenna axes.

To connect the two synchro systems, it was necessary to construct a polar to Cartesian converter to process the MPS-19 radar outputs and change them to x,y,z coordinates for driving the GSN-5. The coordinate converter converts the range, elevation, azimuth data to x,y,z data through potentiometer resolvers. Next, the x,y,z voltage analogs are offset to the GSN-5 position. Another set of resolvers provides an axis rotation to transfer the x,y,z data to the runway coordinate system. Finally, the x data must be converted back to slant range to provide the drive for the GSN-5. This is accomplished in a Cartesian to polar converter.

The main features of the slaving arrangement are shown in the block diagram of Figure 7-2.

B. SLAVING ACCURACY FROM BORESIGHT FILM

Results of various slaving tests of the MPS-19/GSN-5 slaving operation are presented in Table 7-1. These data were obtained from readings of boresight film and the errors shown represent a bias error that remained relatively constant over some period of time.

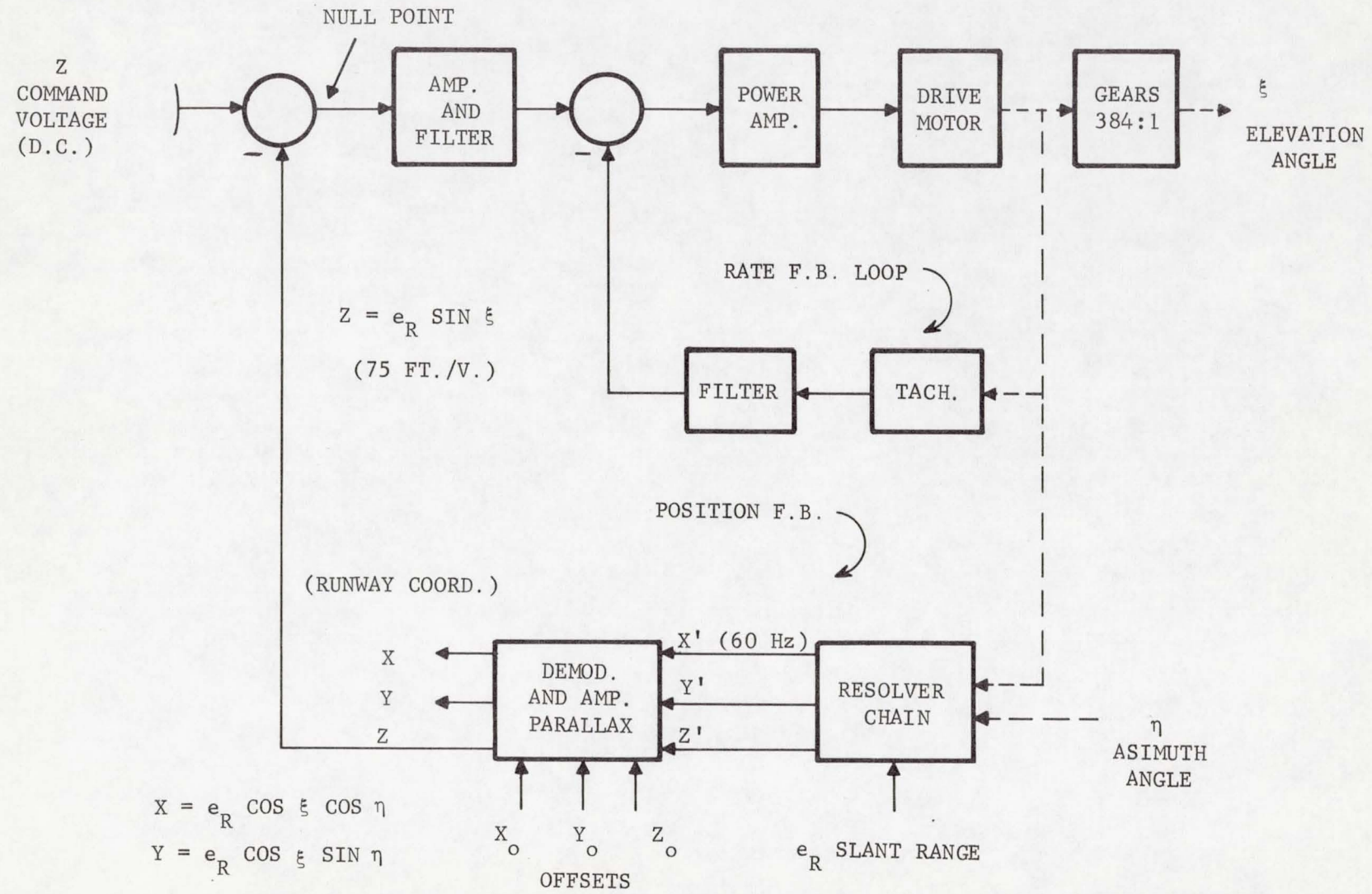

Fig. 7-1. GSN-5 position control servo (El. channel shown).

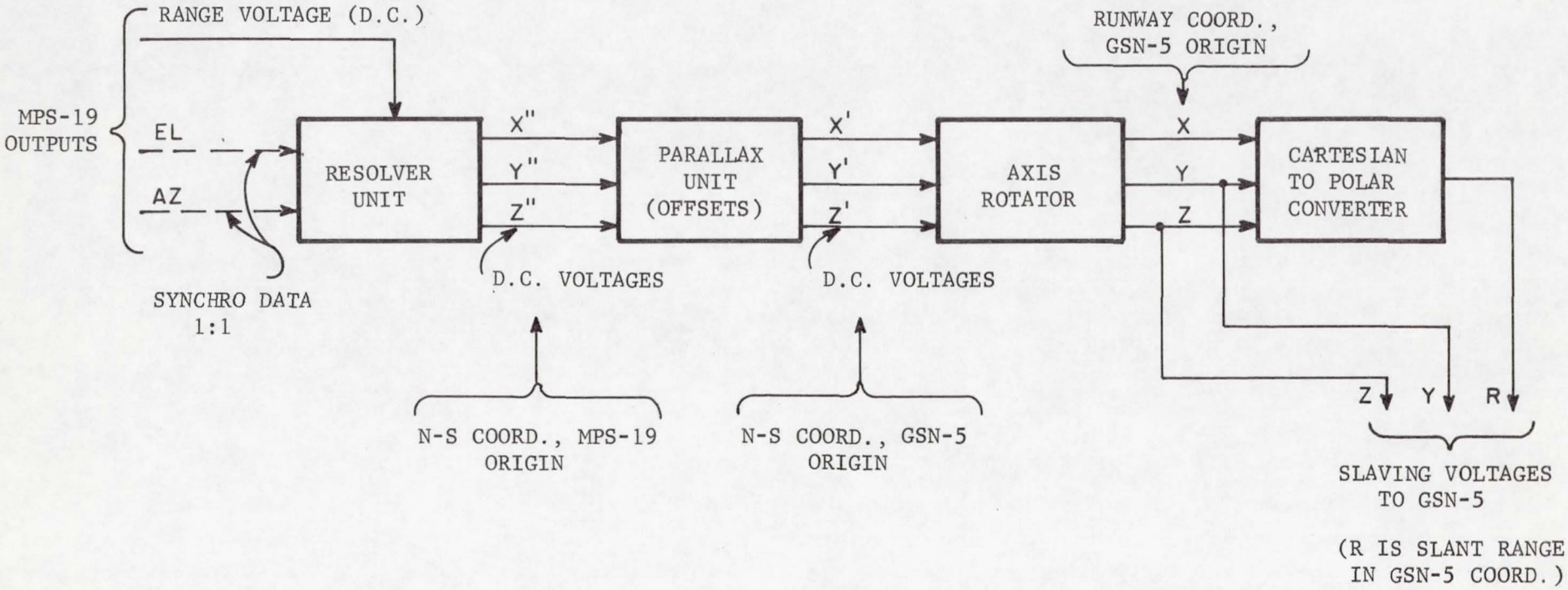

Fig. 7-2. Block diagram of slaving arrangement.

Table 7-1. MPS-19/GSN-5 Slaving Accuracy
(From boresight camera data).

Test and Target	GSN-5 Pointing Errors		GSN-5 Acquisition from Slaving
	Elevation Error[a] (in degrees)	Azimuth Error[a] (in degrees)	
Preliminary Tests (May 23) Helicopter at about 17 Kft. range	-0.34	+1.36	Successful
Preliminary Tests (May 23) Helicopter at about 12.5 Kft. range	-0.31	-direction magnitude >1.8	Unsuccessful
Preliminary Tests (May 23) Helicopter at about 9 Kft. range	-0.37	+1.52	Unsuccessful
Preliminary Tests (May 23) Helicopter at about 5 Kft. range	-0.29	+ direction magnitude >2.0	Unsuccessful
Test 2 - Run A (June 27), C-47 between 6 Kft. and 18 Kft.	Variable between -0.10 and +0.42	Variable between -0.90 and -0.37	Test purposely designed for slaving all the way.
Test 2 - Run A (June 27), C-47 between 3.5 Kft. and 6 Kft.	Variable between +0.42 and +0.97	Variable between -0.60 and -2.00	Test purposely designed for slaving all the way.
Test 2 - Run B (June 27), C-47 at about 26.5 Kft.	Unknown [b]	Unknown [b]	Successful

(Continued on next page.)

Table 7-1. (Continued)

Test and Target	GSN-5 Pointing Errors		GSN-5 Acquisition from Slaving
	Elevation Error /a (in degrees)	Azimuth Error /a (in degrees)	
Test 2 - Run B (June 27), C-47 at about 22.5 Kft.	Unknown /b	Unknown /b	Successful
Test 2 - Run B (June 27), C-47 at about 19.5 Kft.	Unknown /b	Unknown /b	Successful
Test 2 - Run B (June 27), C-47 at about 17 Kft.	- direction magnitude <0.05	-0.31	Successful
Test 2 - Run B (June 27), C-47 between 15 Kft. and 10 Kft.	Continuously Variable between +0.08 and +0.16	Continuously Variable between -0.47 and -1.0	Unsuccessful at 10 Kft. range
Test 2 - Run B (June 27), C-47 at about 4.5 Kft.	+1.0	-1.9	Unsuccessful
Calibration (August 29) Chincoteague Water Tower	-0.26	-1.0	Successful
Test 2 - Run C (August 29)	Not conducted because of slaving loop operational difficulty which was primarily loop oscillation.		

/a For elevation errors, + and - signs indicate the radar pointing above and below, respectively, the target. For azimuth errors, + and - signs indicate the radar pointing to the right and to the left, respectively, of the target.

/b These angles were unknown because the aircraft was beyond camera range.

As indicated in Table 7-1, slaving accuracy was very poor in some cases. Pointing errors in azimuth greater than the 1.4 to 1.5 degrees needed for acquisition were very common. Not shown in the table is a dependence on range in which slaving accuracy tends to worsen with decreasing range. This effect is undoubtedly due to inaccuracies in the parallax correction.

Since the slaving system in practice is almost always used only for acquisition at long ranges, the slaving accuracy problem is not quite as severe as Table 7-1 might lead one to believe. This has been confirmed by the GSN-5 radar operators who state that the system may be operated for several days without failure to achieve acquisition. The degree of slaving accuracy is strongly dependent on the care taken with the setup of the offset correction and calibrations.

During the series of tests outlined in Table 7-1, a complete failure of the slaving system was frequently encountered characterized usually by oscillation of the slaving loop. The suspected cause was marginal gain of the slaving loop and/or noisy slaving inputs from the MPS-19 slaving electronics.

C. SLAVING SWITCHOVER TRANSIENTS

A typical switchover transient (switchover from slave to autotrack and vice versa) is shown in Figure 7-3. The data for this plot were obtained from the boresight film as the system was slaved to the water tower location (X = 23,842 ft, Y = 3,450 ft) and then placed in the autotrack mode. The difference in slaved and locked modes in this case amounted to approximately 1° in azimuth and .26° in elevation.

The transient when going from slaved to lock-on has a well-damped response with small overshoot. This indicates that if the bias errors in slaving could be reduced to the order of .1°, the switchover would be relatively smooth.

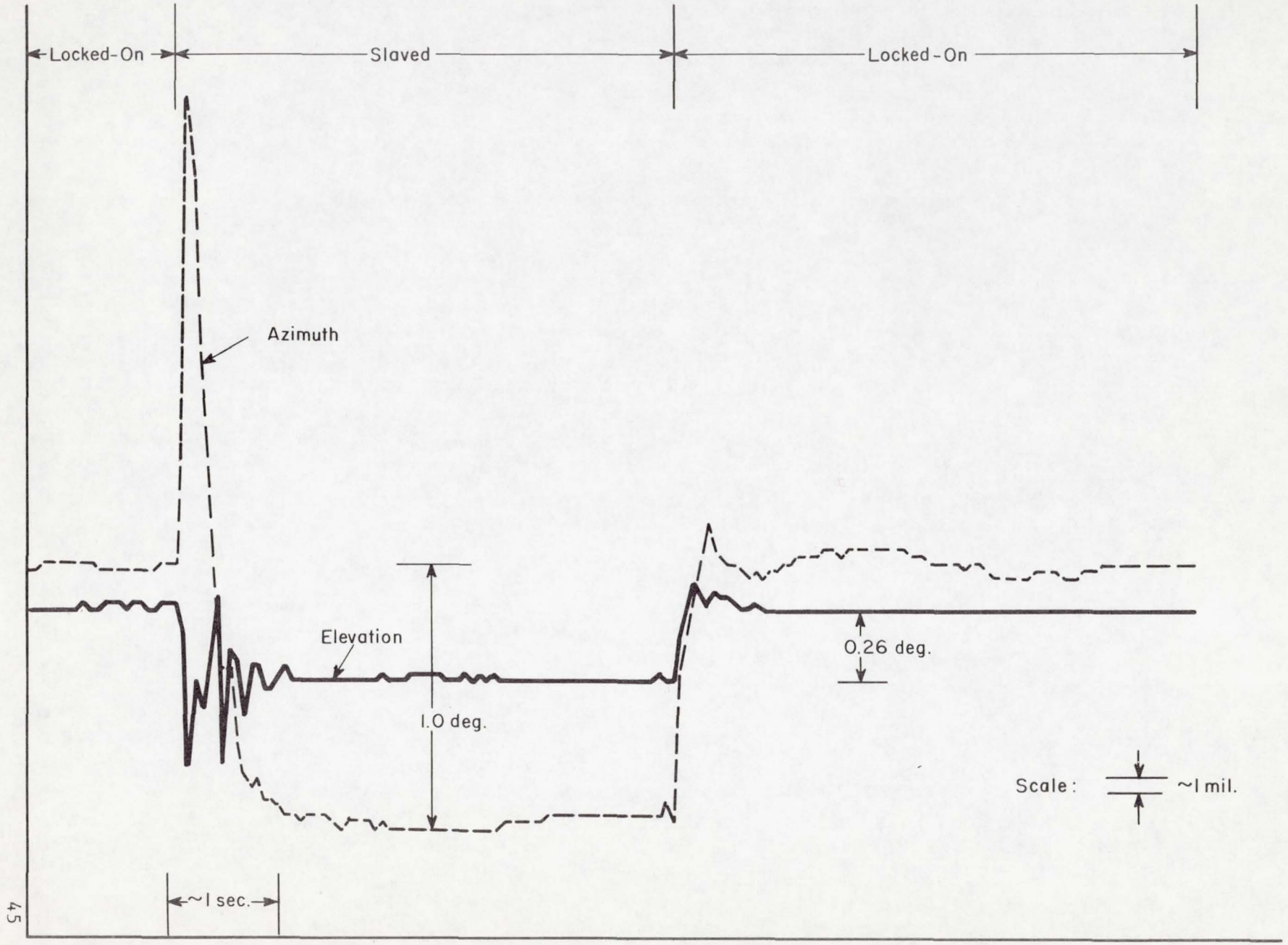

Fig. 7-3. Representative switchover transient (from boresight film).

D. COMPARISON OF MPS-19 AND GSN-5 TRACKS

One data tape was received during which the GSN-5 and MPS-19 were slaved during portions of the run, while in other portions the GSN-5 was in autotrack. The MPS-19 data were transferred to the touchdown coordinate system and compared with GSN-5 outputs. This comparison is shown in Figure 7-4. The portions of the run during which the systems were slaved are indicated on the plots. The large oscillation in the GSN-5 data at about 100 seconds into the run is due to the GSN-5 being in a scan mode.

As may be seen from the data, there are large discrepancies in the coordinate values recorded. In addition, a large transient is evident in the data when switching from autotrack to the slaved mode. These transients actually have a faster response than indicated on the plots since the plots represent data that has been smoothed over approximately 3 seconds. Even though the errors are large, acquisition was successfully achieved during the initial parts of the run. It was not possible to acquire at an elapsed time of approximately 100 seconds, hence the GSN-5 went into the scan mode. Boresight films taken during this run confirm the motions of the antenna as indicated on the plots.

E. MPS-19 ACCURACY

Initial comparison of MPS-19 and FPQ-6 data has been obtained in connection with radar data tape processing at NASA-Wallops. The MPS-19 and FPQ-6 tracking data were differenced for two test runs between ranges of 5,000 and 20,000 feet. Typical values of these differences were:

Table 7-2. MPS-19 and FPQ-6 data differences

Coordinate	Typical Difference
Slant Range	130 to 200 ft.
Azimuth	-.3 to +.2 deg.
Elevation	-.6 to -.7 deg.

GSN-5 X, MPS-19 X, AND DELX VS TIME

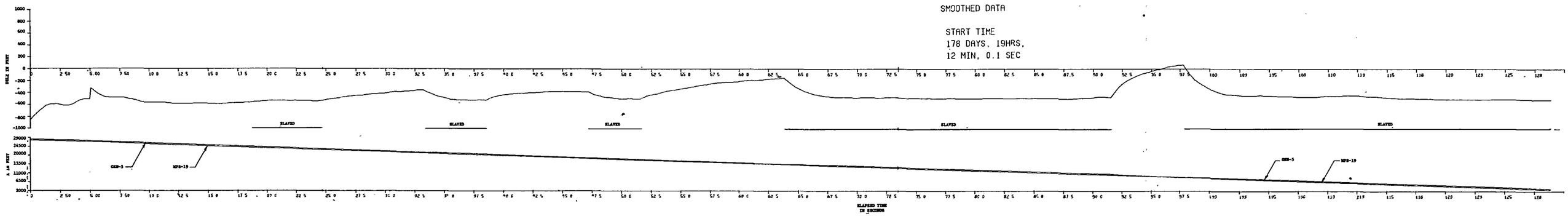

GSN-5 Y, MPS-19 Y, AND DELY VS TIME

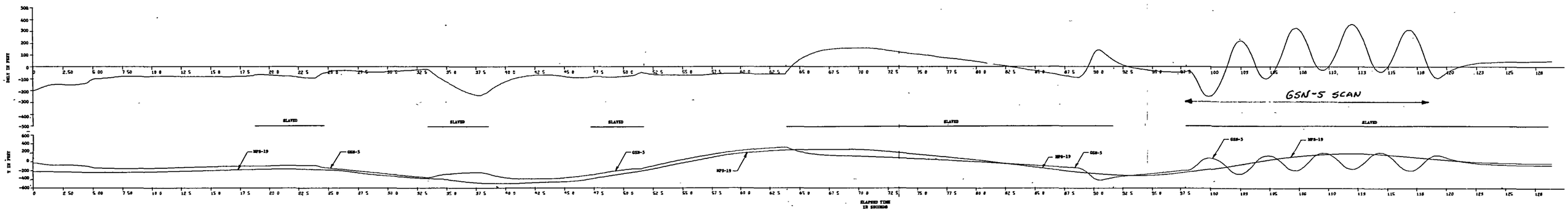

GSN-5 Z, MPS-19 Z, AND DELZ VS TIME

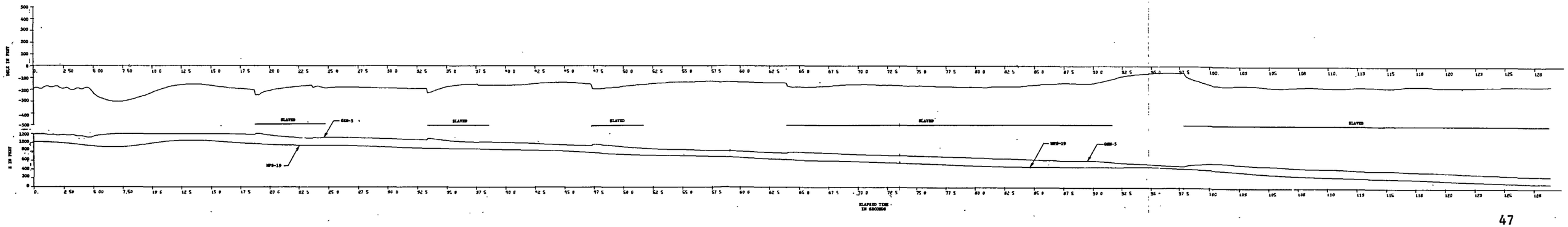

Figure 7-4. Comparison of GSN-5 and MPS-19 data in slaved and tracking modes. Test 2, Run B, June 27, 1969

Even disregarding the elevation results because of possible large differences created by unknown anomalies in the geoid between the FPQ-6 and MPS-19 positions, the azimuth and slant range differences were large compared to the accuracy requirements of the landing radar. Personnel at Wallops are investigating the cause of these large discrepancies. Results of this investigation are not known at the present time.

F. SUMMARY OF SLAVING PERFORMANCE

The slaving performance, while adequate for acquisition at long ranges, does not appear to be performing as well as should be expected. The analog coordinate transformations undoubtedly introduce inaccuracies in the data fed to the GSN-5, but the bias inaccuracies are of the type that could be reduced with careful calibration.

There is an apparent problem in the slaving arrangement as shown in circuit diagrams available at RTI. This problem arises because, if offsets for parallax correction are inserted at the GSN-5 position computer while in the slaved mode, the data required for slaving are X and Y in the runway coordinate system and slant range in a coordinate system with origin at the GSN-5. The data from the MPS-19 are, however, X, Y, and slant range referenced to the GSN-5 position. Thus in this case, the X, Y slaving data from the MPS-19 are in error.

If the parallax offsets are <u>not</u> inserted in the GSN-5 position computer while in the slaved mode, the slaving data from the MPS-19 will be correct, but at switchover to autotrack, the parallax offsets will be inserted and a large transient will appear in the output data.

Another alternative is to reference the data from the MPS-19 to the touchdown coordinate system and leave the offsets in the GSN-5. If this is done, the X,Y data from the MPS-19 will be correct, but slant range will be in error.

Because of operator changeover, we have not been able to determine which of the above techniques was used during the August 29 and June 27 test series. If further GSN-5/MPS-19 slaving is anticipated, modifications should be introduced to correct the apparent flaw in the slaving technique.

VIII. REFERENCES

[1] Handbook for Landing Control, Central, AN/GSN-5, November 1962.

[2] Technical Service Manual, Radar Set AN/MPS-19, Reeves Instrument Corp., T.O. 31P2-2MPS/9-2, March 1957 with changes to 3 December 1962.

IX. APPENDICES

APPENDIX A

COORDINATE TRANSFORMATIONS

For comparing radar measurements the output data of each radar are referred to a common coordinate system. This coordinate system is shown in Figure A-1. Its origin is located at touchdown and its x axis is parallel to the runways. The required transformations for each data type are given below. The radar data types are designated by subscript as follows:

G - Position data for the GSN-5 radar.
M - Position data for the MPS-19 radar.
F - Position data for the FPQ-6 radar.
S - Position data for the MPS-19 slaving output.

The additional subscript T refers to the tracking data as it exists on the radar data tapes.

The available type G data are thus designated $X_{G,T}$, $Y_{G,T}$ and $Z_{G,T}$. The GSN-5 data is already referenced to touchdown and no transformation is required. The coordinates X_G, Y_G, and Z_G are thus simply

$$X_G = X_{G,T}$$

$$Y_G = Y_{G,T}, \text{ and} \qquad \text{(A-1)}$$

$$Z_G = Z_{G,T}.$$

The type M data on the tapes was given in spherical coordinates and is designated as

$$(SR)_{M,T},\ \eta_{M,T},\ \text{and}\ \xi_{M,T}$$

where

$(SR)_{M,T}$ = slant range in feet

$\eta_{M,T}$ = azimuth angle in deg.

$\xi_{M,T}$ = elevation angle in deg.

with the origin already translated to the GSN-5 position (but not to touchdown).

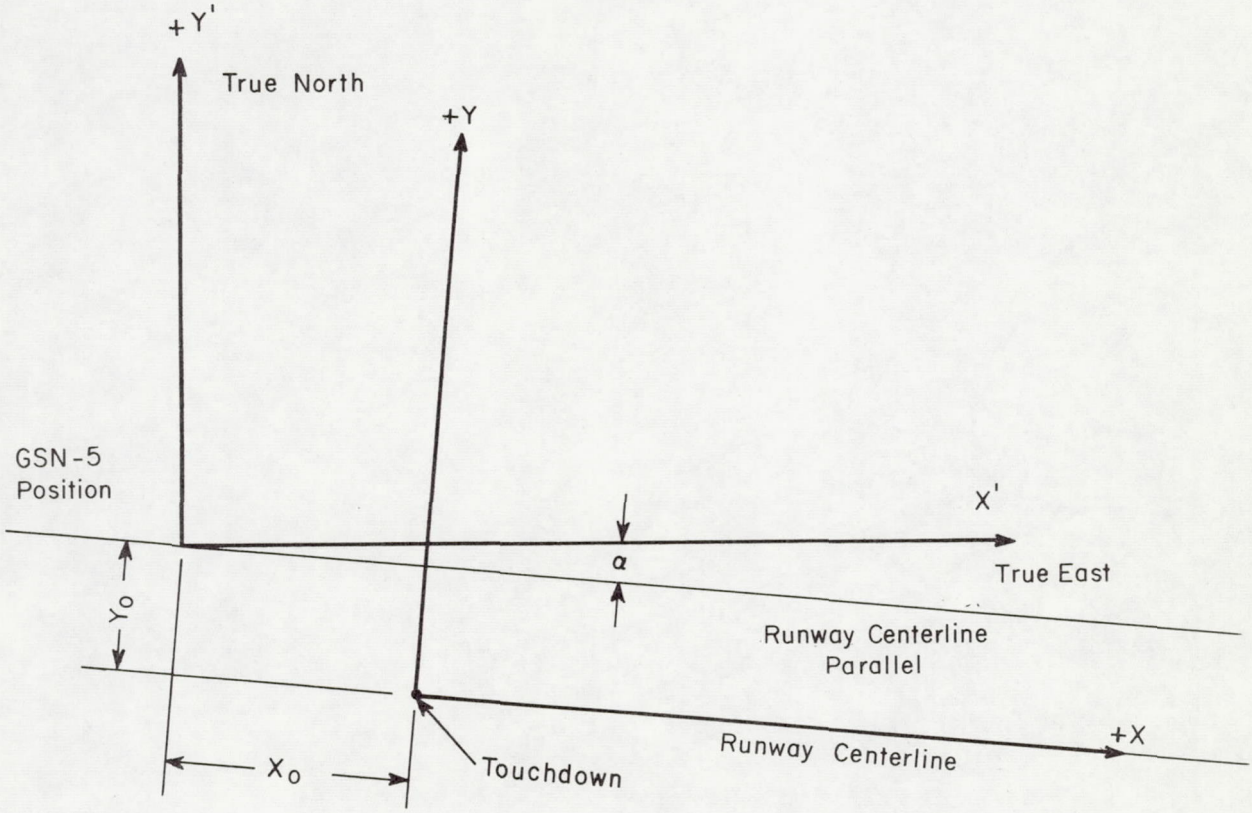

Fig. A-1. Geometry for coordinate transformation.

A straightforward spherical-to-cartesian transformation gives

$$X'_{M,T} = (SR)_{M,T} \cos \xi_{M,T} \sin \eta_{M,T}$$

$$Y'_{M,T} = (SR)_{M,T} \cos \xi_{M,T} \cos \eta_{M,T} \qquad \text{(A-2)}$$

$$Z'_{M,T} = (SR)_{M,T} \sin \xi_{M,T}$$

The x-axis of the reference coordinate system makes an angle α with the east direction and a rotation transformation is therefore required. Rotation plus translation gives rise to the following transformations required for type M data.

$$X_M = \left(X'_{M,T} \cos \alpha\right) - \left(Y'_{M,T} \sin \alpha\right) + X_{M,O}$$

$$Y_M = \left(X'_{M,T} \sin \alpha\right) + \left(Y'_{M,T} \cos \alpha\right) + Y_{M,O} \qquad \text{(A-3)}$$

$$Z_M = Z_{M,T} + Z_{M,O}$$

where α = +0.35556 deg.

$X_{M,O}$ = -723.5 ft.

$Y_{M,O}$ = +257.0 ft.

$Z_{M,O}$ = +7.09 ft.

The <u>type F</u> tracking data was also given in spherical coordinates as

$$(SR)_{F,T} \text{ , } \eta_{F,T} \text{ and } \xi_{F,T}$$

where

$(SR)_{F,T}$ = slant range in feet

$\eta_{F,T}$ = azimuth angle in degrees

$\xi_{F,T}$ = elevation angle in degrees

A spherical-to-cartesian transformation gives

$$X'_{F,T} = (SR)_{F,T} \cos \xi_{F,T} \sin \eta_{F,T}$$

$$Y'_{F,T} = (SR)_{F,T} \cos \xi_{F,T} \cos \eta_{F,T} \qquad \text{(A-4)}$$

$$Z'_{F,T} = (SR)_{F,T} \sin \xi_{F,T}$$

Again rotation plus translation gives the following transformations for type F data.

$$X_F = X'_{F,T} \cos \alpha - Y'_{F,T} \sin \alpha + X_{F,O}$$

$$Y_F = X'_{F,T} \sin \alpha + Y'_{F,T} \cos \alpha + Y_{F,O} \qquad \text{(A-5)}$$

$$Z_F = Z'_{F,T} + Z_{F,O}$$

where

α = +0.35556 deg.

$X_{F,O}$ = -723.5 ft.

$Y_{F,O}$ = +257.0 ft.

$Z_{F,O}$ = +7.09 ft.

The type S data are

$$R_{S,T} \quad Y_{S,T}, \quad Z_{S,T}$$

The appropriate conversions are

$$X_S = R_S \cos \xi_S \cos \eta_S + X_{S,O}$$

$$Y_S = Y_{S,T} + Y_{S,O} \qquad \text{(A-6)}$$

$$Z_S = Z_{S,T} + Z_{S,O}$$

where

$$\xi_S = \sin^{-1}\left(\frac{Z_{S,T}}{R_{S,T}}\right)$$

$$\eta_S = \sin^{-1}\left(\frac{Y_{S,T}}{R_{S,T} \cos \xi_S}\right)$$

$X_{S,O}$ = -723.5 ft.

$Y_{S,O}$ = +257.0 ft.

$Z_{S,O}$ = +7.09 ft.

APPENDIX B

ANALYSIS OF BORESIGHT CAMERA FILM

Reading Methods

Two methods of reading developed film were employed. The second method was used for special cases after it was determined that reading errors and data granularity from the first method were too large in comparison with the pointing errors involved.

The first method involved using a Xerox Microfiche reader (Model No. 1414) to project and enlarge the picture from the film. The image appeared as an approximate 5 in. by 7 in. picture on the reader screen. A transparent grid overlay permitted reading the linear coordinates to the nearest 0.05 inches which with the appropriate conversion was equivalent to a granularity of approximately 0.5 milliradian. This poor resolution, coupled with the inability to consistently position the film (or grid overlay) with good accuracy, required that a better method be used for reading when small variations were to be adequately observed.

The second method involved projection with a 16 mm Bell and Howell analysis parojector located at the Duke University Medical Center. Using an existing setup, the projection created an image approximately 7.5 in. by 10.5 in. Although the image dimensions of this method were only about 40% larger than those of the first method, better illumination permitted a reading resolution of 0.025 inches or approximately 0.16 milliradians, about a three-fold improvement over the first method. Also, the ability to accurately position the image automatically on a frame-by-frame basis gave more consistent readings which considerably decreased the reading error.

Analysis Model for Estimating Pointing Errors

Let the axes (abscissa and ordinate) of the grid system on the projection screen by designated by u and v where u is aligned with the horizontal direction and v with the vertical. The linear position of the target in the projected image can then be read in terms of the units assigned to u and v (inches in this case).

When reading a value for u (or v), some error is present so that

$$u = u_T + \varepsilon_a + \varepsilon_r + \varepsilon_p \qquad \text{(B-1)}$$

where u is the value read, u_T is the true value, ε_a is the inaccuracy due to incorrect positioning of the image (or grid system), ε_r is the error due to reading resolution or data granularity, and ε_p is any error due to optical parallax. It is reasonable to assume that all the variables on the righthand side of Equation B-1 are statistically independent so that

$$\text{Var}\ (u) = \text{Var}\ (u_T) + \text{Var}(\varepsilon_a + \varepsilon_r) + \text{Var}\ (\varepsilon_p) \qquad \text{(B-2)}$$

where Var (·) represents the variance of the quantity in parentheses and the second term of the righthand side is left as the variance of the sum, $\varepsilon_a + \varepsilon_r$, for reasons which will become obvious later.

Rearranging Equation B-2,

$$\text{Var}\ (u_T) = \text{Var}(u) - \text{Var}(\varepsilon_a + \varepsilon_r) - \text{Var}\ (\varepsilon_p) \qquad \text{(B-3)}$$

which shows the variance of the true position to be the variance of the observed value minus the variance of the error. Thus if the variances of the error terms are known or can be estimated to sufficient accuracy they can be subtracted from the estimated variance computed for observed values to obtain an estimate of the variance of the true position. This is the basis for the values of radar RMS (1σ) pointing errors presented in Section IV In particular, the entries in the columns labeled "Description of Value" in Tables 6-1 and 6-2 refer to the various terms in Equation B-1.

Letting k symbolically represent the appropriate conversion factor from inches on the image screen to milliradians in Table 6-1 , the specific meaning of the designations are as follows:

Designation in Tables and	Interpretation
Total Reading	$k\ [\hat{\text{V}}\text{ar}(u)]^{1/2}$
Reading Error	$k\ [\hat{\text{V}}\text{ar}\ (\varepsilon_a + \varepsilon_r)]^{1/2}$
Parallax Contribution	$k\ [\hat{\text{V}}\text{ar}\ (\varepsilon_p)]^{1/2}$
Residual	$k\ [\hat{\text{V}}\text{ar}\ (u_T)]^{1/2}$

where the carat (^) over Var represents the estimated value.

Further description is given below on estimating each of the terms. Note however, that the parallax term applies only to the pointing error in elevation.

Total Reading

For estimating radar pointing errors as presented in Section IV , readings of u and v were taken over 80 consecutive frames (about 5 sec. of tracking time since the film speed was approximately 16 frames per sec.) of selected periods of tracking. For the i-th frame, let the values of u and v be u_i and v_i, respectively. Then the unbiased estimate of the variance of the observed u is

$$\hat{\text{V}}\text{ar}(u) = \frac{1}{79} \sum_{i=1}^{80} (u_i - \bar{u})^2 \qquad \text{(B-4)}$$

where the average, $\bar{u}$, is

$$\bar{u} = \frac{1}{80} \sum_{i=1}^{80} u_i \qquad \text{(B-5)}$$

A similar equation would apply to $\hat{\text{Var}}(v)$

Reading Errors

Separate estimates are obtained for the combined variance of ε_a and ε_r as follows. Suppose that the readings of the first 40 frames were obtained twice so that with the first set of readings, values $u_{1,1},\ldots,u_{40,1}$ are obtained and with the second set, values $u_{1,2},\ldots,u_{40,2}$ are obtained. Consider a pairwise differencing so that

$$\Delta u_i = u_{i,1} - u_{i,2} \qquad \text{(B-6)}$$

From Equation B-1 this gives

$$\Delta u_i = u_{T_{i,1}} + \varepsilon_{a_{i,1}} + \varepsilon_{r_{i,1}} + \varepsilon_{p_{i,1}} - u_{T_{i,2}} - \varepsilon_{a_{i,2}} - \varepsilon_{r_{i,2}} - \varepsilon_{p_{i,2}}$$

Since neither the true value u_T nor the error due to parallax ε_p would change with repeated readings of the same frame,

$$\Delta u_i = \varepsilon_{a_{i,1}} - \varepsilon_{a_{i,2}} + \varepsilon_{r_{i,1}} - \varepsilon_{r_{i,2}}$$

Assuming (reasonably so) that the errors are statistically independent from reading to reading, it follows that

$$\text{Var}(\Delta u) = 2 \text{ Var } (\varepsilon_a + \varepsilon_r)$$

and

$$\text{Var } (\varepsilon_a + \varepsilon_r) = \frac{\text{Var } (\Delta u)}{2}$$

Now from the 40 consecutive differences

$$\text{Var } (\varepsilon_a + \varepsilon_r) = \frac{\text{Var } (\Delta u)}{2} = \frac{1}{2} \left[\frac{1}{39} \sum_{i=1}^{40} (\Delta u_i - \Delta u)^2 \right]$$

where

$$\Delta u = \frac{1}{40} \sum_{i=1}^{40} \Delta u_i$$

Similar relations would also result by similar treatment of the differences in readings for v. Actually, rather than compute separate variance estimates for azimuth and elevation, the statistics were combined to obtain a single estimate considered appropriate for both. The actual computation is

$$\text{Var } (\varepsilon_a + \varepsilon_r) = \frac{1}{2} \left[\frac{1}{79} \sum_{i=1}^{40} (\Delta u_i - \Delta u)^2 + (\Delta v_i - \Delta v)^2 \right] \qquad \text{(B-7)}$$

where the two square terms were verified to be of similar magnitude.

Parallax Contribution

This contributes to the variance of observed pointing errors when the optical axis of the boresight camera is not aligned parallel with the electrical axis of the radar. The boresight camera was mounted vertically above the center of the antenna; therefore, no parallax effect is present in azimuth readings. The geometry for discussing parallax contributions in elevation is presented in Figure B-1. The right and left hand position of the aircraft represent respectively the initial and final position of the target for the 5 sec. data interval over which the boresight film is read to compute pointing errors. The image screen is superimposed on the

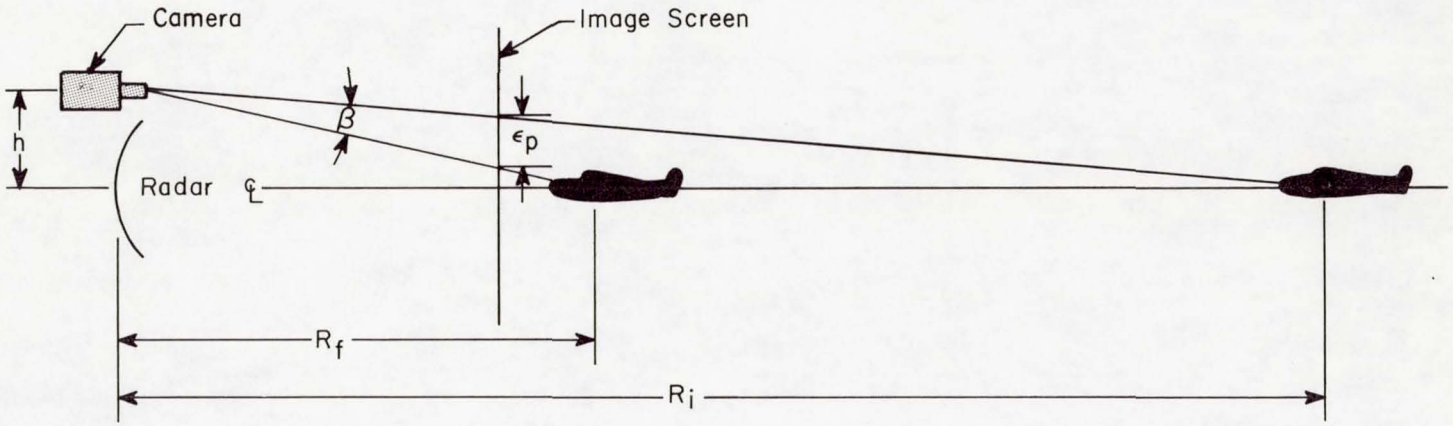

Figure B-1. Geometry for illustrating parallax contributions to observed radar pointing errors.

geometry to illustrate the movement of the optical camera position during this time period. β is the angle of interest corresponding to the total distance of movement of the target on the screen.

Assuming that the angles between the optical line-of-sight and the radar centerline are always small (which they are for all geometries in question), it is easily shown that

$$\beta = h\left(\frac{R_i - R_f}{R_i R_f}\right) \text{ in radians.} \qquad \text{(B-8)}$$

Now β represents the maximum change of an angle $\theta(t)$ which during the time interval in question varies, for all practical purposes, linearly with time so that

$$\theta(t) = \frac{\beta}{T} t.$$

The variance contributed by $\theta(t)$ to readings in vertical angular pointing error is simply the second moment of $\theta(t)$ about the mean in this interval which is

$$\text{Var}(\theta(t)) = \frac{1}{T} \int_0^T \left(\frac{\beta}{T} t - \overline{\theta}\right)^2 dt = \frac{\beta^2}{12}$$

Substituting Equation B-8 into this expression yields

$$\text{Var}(\theta(t)) = \frac{h^2}{12} \left[\frac{R_i - R_f}{R_i R_f}\right]^2 \qquad \text{(B-9)}$$

which from known geometry can be used to compute the parallax contribution directly. As indicated in Tables 6-1 and 6-2, the effect is negligible at the longer ranges but needs to be included at short ranges.

For one case in Tables 6-1 and 6-2 , viz., the beacon track case at short range, another parallax effect was present. This resulted because a

reference point on the aircraft was used for reading convenience which was displaced vertically from the actual target, the beacon antenna. Since calculations of this effect are similar, they are not shown. This contribution was almost precisely the same magnitude but of opposite sign which as shown in Tables 6-1 and 6-2 rendered the overall contribution negligible for this case.

APPENDIX C

SYSTEM ERROR ANALYSIS

A diagram of the recording system for the GSN-5 radar x output showing possible sources of error is presented in Fig. C-1. Similar diagrams would apply to the other output variables recorded. The overall input/output relation for the system is also given in Fig. C-1. This relation is presented in terms of general gain and error symbols. More detailed consideration follows for reducing this equation to a practical error analysis formula and for explaining the various sources of error, how they are treated in the analysis, and how they affect the results.

Calibration

To achieve the correct scaling of the output data, calibrations were conducted on the latter part of the system between the recorder input voltages e_a and output x_c. This consisted merely of applying d.c. inputs at various levels to the recorder and using the digital output data to establish the necessary relation between input and output.

With reference to Fig. C-1 the input/output relation for the part of the system in consideration is seen to be

$$x_c = (G_p + \gamma_p)(G_c + \gamma_c) E_a + (G_c + \gamma_c) \varepsilon_p + \varepsilon_c \qquad \text{(C-1)}$$

where E_a is substituted for e_a to denote a d.c. input and other symbols are as defined in the figure. ε_p, the error introduced in the recording and playback portion, is considered composed of a possible d.c. bias E_p plus an a.c. noise component $N_p(t)$ so that

$$\varepsilon_p = E_p + N_p(t) \qquad \text{(C-2)}$$

For brevity we let

$$G_1 = (G_p + \gamma_p)\ (G_c + \gamma_c)$$

and

$$G_2 = (G_c + \gamma_c)$$

so that eq. (C-2) can be expressed as

$$x_c = G_1 E_a + G_2 E_p + G_2 N_p(t) + \varepsilon_c. \qquad \text{(C-3)}$$

To determine the appropriate scaling of the output, the output values obtained for each several seconds of input d.c. are averaged and these average values used to establish a calibration plot of $\bar{x}_c$, the average value of x_c, versus E_a. For the averaging process $N_p(t)$ is assumed to have a zero mean. Also, ε_c represents the error due to digital granularity and as discussed in later text is assumed to have a zero mean. Therefore, averaging both sides of eq. (C-3) gives

$$\bar{x}_c = G_1 E_a + G_2 E_p \qquad \text{(C-4)}$$

where the averages of E_a and E_p are expressed as the quantities themselves since they are d.c. terms. Thus by virture of eq. (C-4) one would expect the calibration function to be a linear function of E_a with an offset from the origin.

Plotted values of $\bar{x}_c$ computed from output data typically fell within ± 1% of an "eye-fitted" straight line through the points; however, it was decided that a more accurate representation of the calibration function is a piecewise linear function obtained by linear interpolation between points.

The uncertainty in $\bar{x}_c$ due to possible input voltage errors and sampling variability and its effect on calibration is discussed in Appendix C.

Note that when $E_a = 0$ in eq. (C-4),

$$\bar{x}_c \Big|_{E_a = 0} = G_2 E_p \tag{C-5}$$

which represents the bias in the calibration function if it were truly linear and which could be estimated for the condition $E_a = 0$. Thus any bias introduced in the recording and playback system can be estimated and removed. This is represented symbolically in Fig. C-1 by the last summing point in the diagram; however, in actuality this removal of bias is taken care of automatically in the linear interpolation scheme for generating the piecewise linear representation. The net result in either case is to express the final output simply as

$$\bar{x}_o = G_1 E_a. \tag{C-6}$$

Substituting the earlier expression for G_1 and returning to the appropriate notation for test data,

$$x_o = (G_p + \gamma_p)\ (G_c + \gamma_c)\ e_a \tag{C-7}$$

or

$$e_a = \frac{x_o}{(G_p + \gamma_p)\ (G_c + \gamma_c)} \tag{C-8}$$

Also, from the first part of the system

$$e_a = G_r G_a x_T \tag{C-9}$$

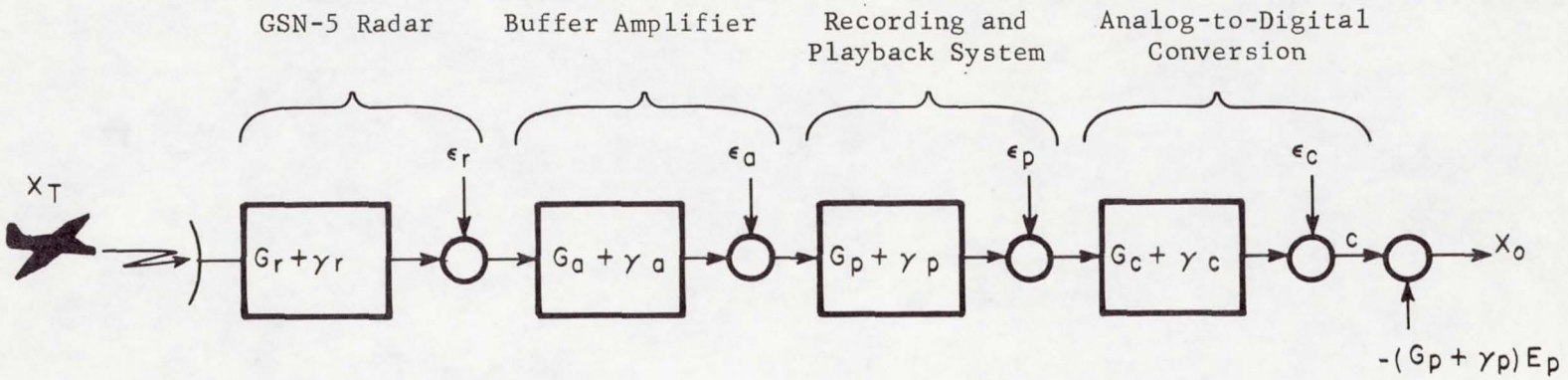

Legend

x	=	position coordinate	Subscript r denotes the GSN-5 radar
G	=	component nominal gain	Subscript a denotes the buffer amplifier
γ	=	error in component gain	Subscript p denotes the recording and playback system
e	=	tracking output signal	Subscript c denotes the A/D conversions
ϵ	=	additive error in a component	Subscript o denotes the system output
E_p	=	predetermined d.c. component of ϵ_p	Subscript T denotes the target or aircraft

Input/Output Relation

$$x_o = (G_r + \gamma_r)(G_a + \gamma_a)(G_p + \gamma_p)(G_c + \gamma_c)\, x_T + (G_a + \gamma_a)(G_p + \gamma_p)(G_c + \gamma_c)\, \epsilon_r + (G_p + \gamma_p)(G_c + \gamma_c)\, \epsilon_a$$

$$+ (G_c + \gamma_c)\, \epsilon_p + \epsilon_c - E_p(G_c + \gamma_c)$$

Fig. C-1. GSN-5 radar tracking and recording system for error analysis.

under nominal gain and zero error conditions. By equating eqs. (C-8) and (C- 9) it is easily seen that $x_o = x_T$ only when

$$(G_p + \gamma_p)\ (G_c + \gamma_c) = \frac{1}{G_r G_a} \tag{C-10}$$

Therefore, regardless of the errors in the gains of the recording and playback system and the A/D conversion, they can be set by calibration to remove these sources of error.

The Error Equation

Similar to eq. (C-1) for ε_p, the error terms ε_r and ε_a are also expanded into d.c. bias and a.c. noise, as

$$\varepsilon_r = E_r + n_r(t) \tag{C-11}$$

and

$$\varepsilon_a = E_a + n_a(t) \tag{C-12}$$

Now using the general input/output relation given in Figure C-1 and substituting eqs. (C-2) and (C-10) through (C-12), the output can be expressed as

$$x_o = x_T + \frac{\gamma_r}{G_r} x_T + \frac{\gamma_a}{G_a} x_T + \frac{E_r}{G_r} + \frac{n_r(t)}{G_r} + \frac{E_a}{G_a G_r} + \frac{n_a(t)}{G_a G_r} + N_p(t) + \varepsilon_c \tag{C-13}$$

where terms containing products of errors are ignored since their contribution would be extremely small and where

$$N_p(t) = (G_c + \gamma_c)\ N_p(t) \tag{C-14}$$

Similar expressions would also apply to other GSN-5 radar output variables such as y and z.

The usual intent in the development of an error model such as Eq. C-13 is the analysis of the contribution of each error source to the variability or uncertainty in the result. Because of extensive low frequency noise introduced by the recorder (equivalently the $n_r(t)$ term in eq. (C-13)) and the extensive data smoothing required to suppress it, the utility of Eq. C-13 is limited in this case only to analysis of fixed biases and extremely slow variations. Specifically, the data smoothing was designed to provide at least 10 db suppression of 0.33 Hz oscillations. For practical purposes, the data smoothing thus reduces the error model to

$$x_o = x_T + \frac{\gamma_r}{G_r} x_T + \frac{\gamma_a}{G_a} x_T + \frac{E_r}{G_r} + \frac{E_a}{G_a G_r} \qquad \text{(C-15)}$$

For further simplification it is noted that the chopper stabilization of the buffer amplifiers and the precision balancing available renders the last term in Eq. (C-15) negligible. Dropping this term and rearranging,

$$x_o - x_T = \frac{\gamma_r}{G_r} x_T + \frac{E_r}{G_r} + \frac{\gamma_a}{G_a} x_T. \qquad \text{(C-16)}$$

Thus all the error in the output following data smoothing is thus due to the error in gain and bias of the radar plus the error in gain of the buffer amplifier. Actual measurements of gain during the August 29 tests showed that amplifier gain variations over a period of several hours (i.e., drift in gain) was negligible. Furthermore, these measurements of amplifier gain rendered the last term in Eq. (C-16) zero for data recorded on that date since gain was thus known without error. Therefore, Eq. (C-16) reduces to

$$x_o - x_T = \frac{\gamma_r}{G_r} x_T + \frac{E_r}{G_r} \qquad \text{(C-17)}$$

which shows all of the error in the output to be due to the radar. These data also showed that the worst case departure of amplifier gain from the nominal value was 0.4%,* a figure which can reasonably be expected to apply to data taken on earlier test dates. Thus the maximum error in x_o due to error in amplifier gain when $x_T = 100$ is estimated as 0.4 ft. Note however, that worst case errors in y and z near touchdown would be even less since both y and z would be much less than 100 feet.

*The RMS deviation computed from ten independent readings was 0.33%.

APPENDIX D

RECORDING AND PLAYBACK SYSTEM FOR RADAR ANALOG OUTPUTS

To facilitate data processing of radar data, provision was made to store radar outputs on magnetic tape for later analog-to-digital conversion. The recording system is illustrated in Fig. D-1 showing the specific variables recorded.

The buffer amplifiers were required to drive the recorder channels. These amplifiers were operational amplifiers (chopper stabilized vacuum tube type) contained in a portable Donner analog computer (Model 3400). The dynamic range of ±100 volts from the GSN-5 radar also had to be reduced to ±10 volts for compatibility with the recorder input requirements, and using the operational amplifiers with selectable input and feedback resistances provided a convenient way of achieving this gain modification.

The FM tape recorder was a fourteen channel Ampex unit operated with a 54 KHz carrier, 40% maximum frequency deviation, and 30 inches per second tape speed. As noted in the main body of this report, considerable low frequency noise was encountered in the system which, based on available evidence, was felt certain to be due to variations in tape speed.

The strip chart recorder was the light beam galvanometer deflection type. These recordings were used primarily to indicate what data was contained on the magnetic tape.

Playback and conversion of the data to digital form was performed at the NASA Langley Data Reduction Center. A simplified block diagram of the process is illustrated for a single channel in Fig. D-2. Sampling rates for the analog-to-digital conversion were standardized at 10 samples per second thus preserving an effective signal bandwidth of approximately 5 Hz. The low pass filter was included in the system to reject any wideband noise introduced by the recording system and prevent possible aliasing effects in the sampling process. Available filters permitted cutoff

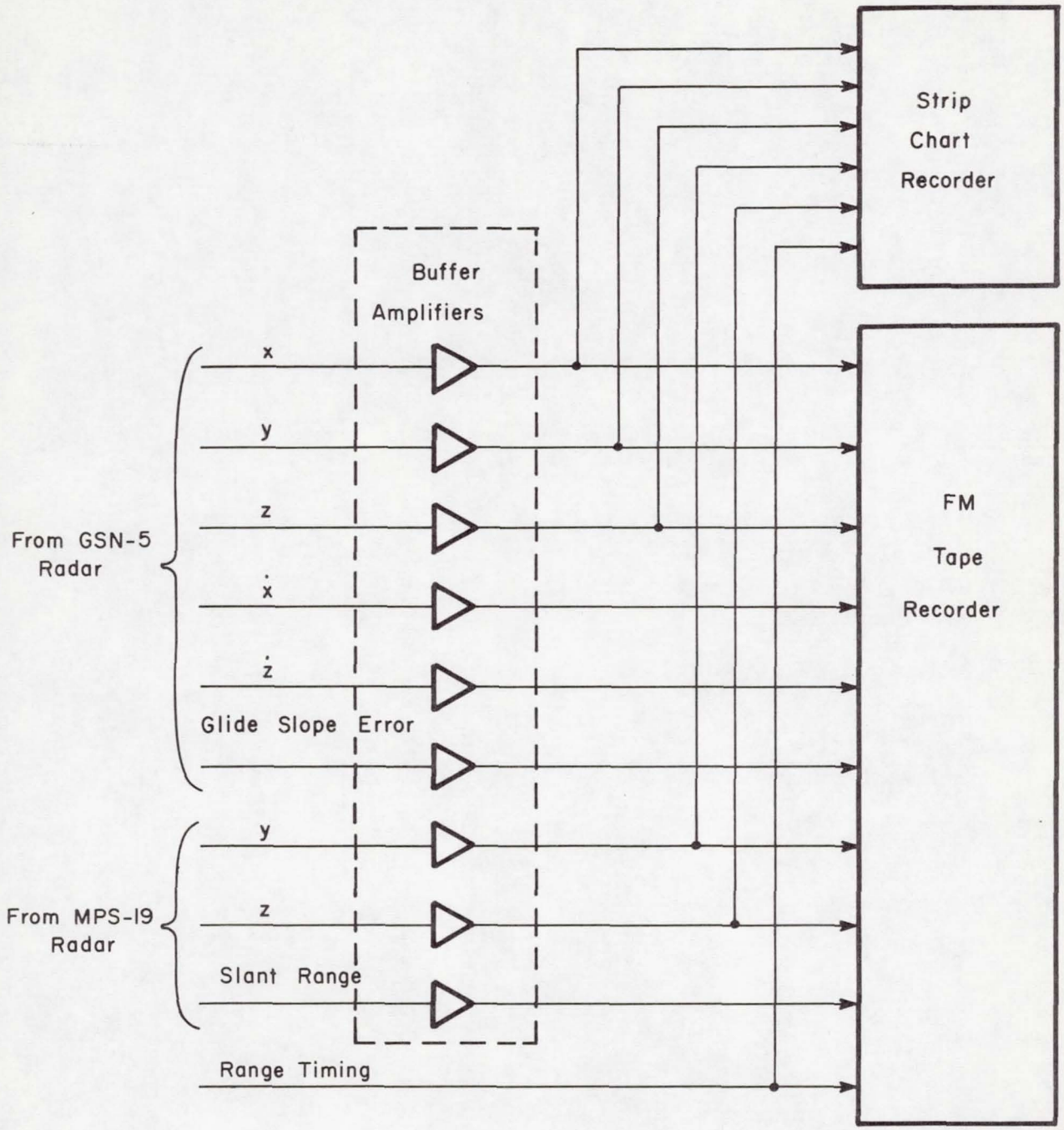

Figure D-1. System for recording radar analog outputs.

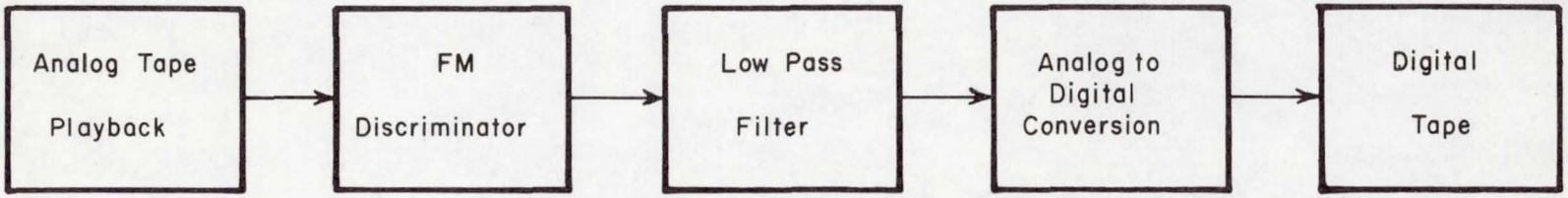

Fig. D-2. Playback and analog-to-digital conversion for a single channel.

frequencies in the range from 20 to 50 Hz. It is important to note that much of the recorder noise was at frequencies lower than 5 Hz,thus remained in the converted data.

APPENDIX E

SURVEY DATA

Figure E.1 indicates the surveyed positions of the MPS-19 and GSN-5 radars relative to the runway and touchdown point (station 8). The +Y coordinate points approximately north. All tests were conducted with the aircraft landing from East to West.

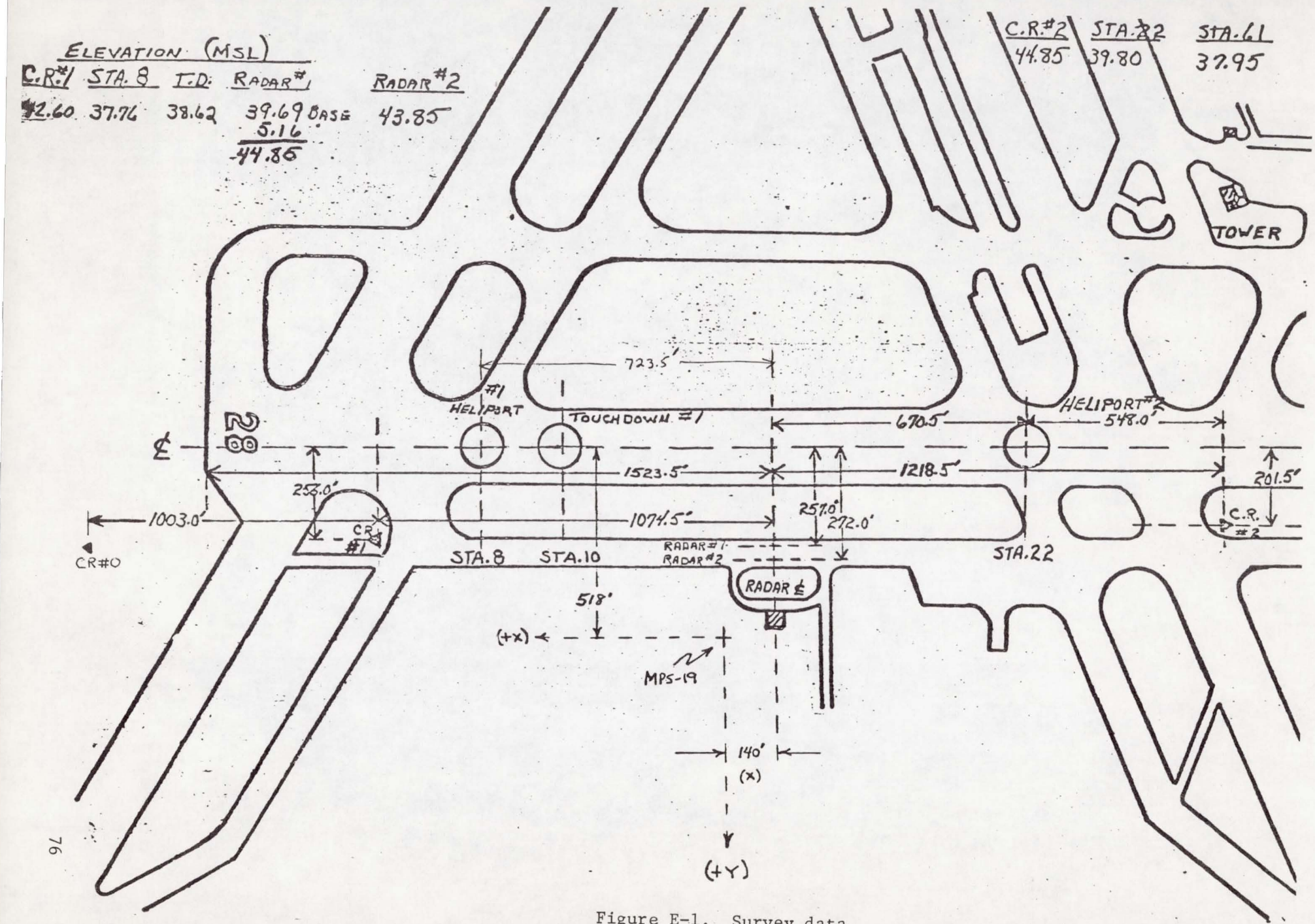

Figure E-1. Survey data.